

University of Groningen

Targeted epigenetic editing of SPDEF reduces mucus production in lung epithelial cells

Song, Juan; Cano-Rodriguez, David; Winkle, Melanie; Gjaltema, Rutger A. F.; Goubert, Désirée; Jurkowski, Tomasz P.; Heijink, Hilde; Rots, Marianne; Hylkema, Machteld

Published in:

American Journal of Physiology - Lung Cellular and Molecular Physiology

DOI:

[10.1152/ajplung.00059.2016](https://doi.org/10.1152/ajplung.00059.2016)

IMPORTANT NOTE: You are advised to consult the publisher's version (publisher's PDF) if you wish to cite from it. Please check the document version below.

Document Version

Final author's version (accepted by publisher, after peer review)

Publication date:

2017

[Link to publication in University of Groningen/UMCG research database](#)

Citation for published version (APA):

Song, J., Cano-Rodriguez, D., Winkle, M., Gjaltema, R. A. F., Goubert, D., Jurkowski, T. P., ... Hylkema, M. N. (2017). Targeted epigenetic editing of SPDEF reduces mucus production in lung epithelial cells. *American Journal of Physiology - Lung Cellular and Molecular Physiology*, 312(3), L334-L347. DOI: 10.1152/ajplung.00059.2016

Copyright

Other than for strictly personal use, it is not permitted to download or to forward/distribute the text or part of it without the consent of the author(s) and/or copyright holder(s), unless the work is under an open content license (like Creative Commons).

Take-down policy

If you believe that this document breaches copyright please contact us providing details, and we will remove access to the work immediately and investigate your claim.

Downloaded from the University of Groningen/UMCG research database (Pure): <http://www.rug.nl/research/portal>. For technical reasons the number of authors shown on this cover page is limited to 10 maximum.

1 **Targeted epigenetic editing of SPDEF reduces mucus production in lung epithelial**
2 **cells**

3 Juan Song^{1,2,3}, David Cano Rodriguez¹, Melanie Winkle¹, Rutger A.F. Gjaltema¹, Désirée
4 Goubert¹, Tomasz P. Jurkowski⁴, Irene H. Heijink^{1,2}, Marianne G. Rots^{1,*} and Machteld N.
5 Hylkema^{1,2,*}

6 ¹University of Groningen, University Medical Center Groningen, Department of Pathology
7 and Medical Biology, Groningen, the Netherlands

8 ²University of Groningen, University Medical Center Groningen, GRIAC Research Institute,
9 Groningen, the Netherlands

10 ³Tianjin Medical University, School of Basic Medical Sciences, Department of Biochemistry
11 and Molecular Biology, Department of Immunology, Tianjin, China

12 ⁴Institute of Biochemistry, Pfaffenwaldring 55, Faculty of Chemistry, University of Stuttgart,
13 D-70569 Stuttgart, Germany

14 * These authors contributed equally to this work.

15

16 **Correspondence:** Machteld Hylkema, PhD

17 Department of Pathology and Medical Biology EA10, University Medical Center Groningen,
18 Hanzeplein 1, 9713 GZ Groningen, the Netherlands

19 Phone: 00 31 50 3619850. Fax: 00 31 50 3619107. E-mail: m.n.hylkema@umcg.nl

20 **Keywords:** *SPDEF*, epigenetic editing, mucus production, DNA methylation

21 **Running title:** Epigenetic silencing of *SPDEF* reduces MUC5AC production

22

23 **Abstract**

24 Airway mucus hypersecretion contributes to the morbidity and mortality in patients with
25 chronic inflammatory lung diseases. Reducing mucus production is crucial for improving
26 patients' quality of life. The transcription factor SAM-pointed domain-containing Ets-like
27 factor (*SPDEF*) plays a critical role in the regulation of mucus production, and therefore
28 represents a potential therapeutic target. This study aims to reduce lung epithelial mucus
29 production by targeted silencing *SPDEF* using the novel strategy epigenetic editing.
30 Zinc fingers and CRISPR/dCas platforms were engineered to target repressors (KRAB, DNA
31 methyltransferases, histone methyltransferases) to the *SPDEF* promoter.
32 All constructs were able to effectively suppress both *SPDEF* mRNA and protein expression,
33 which was accompanied by inhibition of downstream mucus-related genes (Anterior
34 gradient 2 (*AGR2*), Mucin 5AC (*MUC5AC*)). For the histone methyltransferase G9A, and not
35 its mutant nor other effectors, the obtained silencing was mitotically stable.
36 These results indicate efficient *SPDEF* silencing and down regulation of mucus related gene
37 expression by epigenetic editing, in human lung epithelial cells. This opens avenues for
38 epigenetic editing as a novel therapeutic strategy to induce long-lasting mucus inhibition.
39

40 **Introduction**

41 Airway epithelial mucus secretion and mucociliary clearance plays a key role in protective
42 innate immune responses against inhaled noxious particles and microorganisms. However,
43 excessive mucus production and secretion contributes to the pathogenesis of several
44 chronic inflammatory lung diseases such as asthma and chronic obstructive pulmonary
45 disease (COPD) (9, 11, 27). In patients with asthma and COPD, mucus hypersecretion is
46 associated with cough and sputum production, respiratory infections, accelerated lung
47 function decline, exacerbations and mortality (23, 34). Therefore, targeted treatment of
48 pathologic airway mucus secretion is expected to not only improve symptoms of cough and
49 dyspnea, but also decrease the frequency of disease-related exacerbations and decelerates
50 the disease progression. In the past few years, in preclinical models relevant to COPD,
51 several drugs were shown to reduce mucus hypersecretion (21). However, none of these
52 drugs targeted the mucus producing cell itself.

53 Airway mucus contains mostly water and secreted mucins that contribute to the viscosity
54 and elasticity of mucus gels. Mucin 5AC (*MUC5AC*) is the major secreted mucin, which is
55 mainly produced by goblet cells in the airway epithelium. In chronic respiratory diseases,
56 mucus hypersecretion is highly associated with increased numbers of goblet cells, as well as
57 up regulated levels of mucin synthesis and secretion (9). SAM pointed domain-containing
58 Ets transcription factor (*SPDEF*) has been reported to be a core transcription factor (TF) that,
59 within a large network of genes, controls mucus production and secretion (6, 22, 35). In
60 lung, *SPDEF* is selectively expressed in goblet cells lining the airways of patients with chronic
61 lung disease (6) and mice exposed to allergens (25). In mice, the absence of *SPDEF* was
62 shown to protect from goblet cell development after allergen exposure (6, 26). Moreover,

63 knockdown of *SPDEF* with small interfering RNA (siRNA) was found to significantly reduce
64 the expression of IL-13-induced *MUC5AC* expression and Anterior gradient 2 (*AGR2*)
65 expression, which encodes a potential chaperone required for mucin packaging, in the
66 human bronchial epithelial cell line 16HBE (36). These observations suggest that *SPDEF*
67 could be a potential therapeutic target of airway mucus hypersecretion. In this study we set
68 out to silence *SPDEF* expression by epigenetic editing. Epigenetic editing is a novel approach
69 to modulate epigenetic states locally by targeting an epigenetic enzyme to the locus of
70 interest via DNA-targeting systems, such as zinc fingers (ZFs), transcription activator-like
71 effectors (TALEs), or clustered regularly interspaced short palindromic repeats (CRISPRs) (5,
72 8, 17, 33). Compared to artificial transcription factors (ATFs), which exploit programmable
73 DNA-binding platforms to target transcriptional activators or repressors with no catalytic
74 domain (such as super KRAB Domain, SKD), epigenetic editing has the promise to induce
75 stable and inheritable gene modulation (4, 31). In this study, we provide proof-of-concept
76 that *SPDEF* provides a promising target for epigenetic editing to prevent epithelial *MUC5AC*
77 expression.

78

79 **Materials and Methods**

80 **Cell culture**

81 Human bronchial epithelial 16HBE 14o- (16HBE) and BEAS-2B, mucoepidermoid carcinoma
82 NCI-H292 and type II alveolar carcinoma A549 cell lines were cultured as previously
83 described (15). The human embryonic kidney HEK293T cell line (obtained from American
84 Type Culture Collection (ATCC)) and the breast cancer cell line MCF7 (obtained from ATCC:
85 HTB-22) were cultured in Dulbecco's modified Eagle medium (Biowhittaker, Verviers,

86 Belgium). All culture media were supplemented with 2 mmol/L L-glutamine, 50 µg/mL
87 gentamicin, and 10% FBS (Biowhittaker).

88

89 **Plasmids Constructs**

90 Four 18-bp zinc finger (ZF) protein target sites were selected within the *SPDEF* promoter
91 using the website www.zincfingertools.org, as previously described (16). The target
92 sequences are shown in Fig. 2a. The DNA sequences encoding the ZFs were synthesized by
93 Bio Basic Canada. The fragments encoding the ZFs were digested with BamHI/ NheI
94 restriction enzymes (Thermo Fisher Scientific, Carlsbad, USA) and cloned into a SKD-NLS-ZF-
95 TRI FLAG backbone, which encodes SKD, a triple-FLAG tag and a nuclear localization signal
96 (NLS) or a ZF- NLS-VP64-TRI FLAG backbone, which encodes a tetramer of Herpes Simplex
97 Virus Viral Protein 16 (VP64). Then the SKD-NLS-ZF SPDEF-TRI FLAG fragments and the ZF
98 SPDEF- NLS-VP64-TRI FLAG were XbaI/ NotI (Thermo Fisher Scientific) digested and
99 subcloned into a dual promoter lentiviral vector pCDH-EF1-MCS-BGH PCK-GFP-T2A-Puro
100 (SBI, Cat. #CD550A-1), obtaining constructs CD550A-1 SKD-ZF SPDEF and CD550A-1 ZF
101 SPDEF-VP64. To obtain the constructs CD550A-1 ZF SPDEF-DNMT3A, the DNMT3A catalytic
102 domain (kindly provided by Dr. A Jeltsch) was digested out from pMX-ZF-DNMT3A-IRES-GFP
103 with AscI and PacI, to replace VP64 in the CD550A-1 ZF SPDEF-VP64 vector. Catalytically
104 mutant of DNMT3A (E74A) (13) was generated by PCR-mediated site directed mutagenesis
105 on CD550A-1 ZF SPDEF-DNMT3A. To obtain the constructs CD550A-1 ZF SPDEF-G9a and
106 CD550A-1 ZF SPDEF-G9a W1050A, the G9a catalytic domain and its mutant was digested out
107 from pMX-E2C-G9a and pMX-E2C-G9a W1050A (10) with AscI and PacI, to replace VP64 in
108 the CD550A-1 ZF SPDEF-VP64. To construct the CD550A-1 ZF SPDEF without effector

109 domains (EDs) (SPDEF-NOED), VP64 in the CD550A-1 ZF SPDEF-VP64 was swapped out with
110 PCR by a multiple cloning site, including restriction sites for *Ascl*, *Nsil*, *BclI*, *SwaI*, and *PacI*.
111 The primer information is presented in Table 1. pHAGE EF1 α dCas9-VP64 lentiviral construct
112 was a gift from Rene Maehr & Scot Wolfe (Addgene plasmid # 50918)(18) and the single-
113 chain guide RNA encoding plasmid MLM3636 was a gift from Keith Joung (Addgene plasmid
114 # 43860). An additional multiple cloning site was added by replacing the VP64 activator with
115 a sequence containing a *MluI* restriction site. To obtain the dCas9-epigenetic editor
116 constructs, the G9a catalytic domain and its mutant, the SUV39h1 catalytic domain (10), and
117 the catalytic domain of EZH2 (SET) and its mutant were digested out from pMX-ZF-IRES-GFP
118 with *MluI* and *NotI* and subcloned into the empty pHAGE EF1 α dCas9. The SKD domain and
119 the DNMT3A3L catalytic domain and its catalytic mutant (29) were subcloned by amplifying
120 with primers containing *MluI* and *NotI* overhangs. Cloning of guide RNAs (gRNA) was
121 achieved as previously described (4). Briefly, pairs of DNA oligonucleotides encoding 20
122 nucleotide gRNA targeting sequences were annealed together to create double-stranded
123 DNA fragments with 4-bp overhangs. These fragments were ligated into *BsmBI*-digested
124 plasmid pMLM3636. Two gRNAs were designed to bind close to the region where ZF3 and
125 ZF4 bind (Fig. 2A) (GCATGGATCCCCAGCAAGG and CCTCAGGTTGGCCTTGCCA,
126 respectively) and a third gRNA was designed to bind just before transcription start site
127 (CTGGCCAACTTTCATCTCG). We verified all constructs by DNA Sanger sequencing
128 (Baseclear, Leiden, the Netherlands).

129

130 **Lentiviral transduction**

131 The lentiviral CD550A-1 constructs, encoding the *SPDEF* targeting ATFs and epigenetic
132 editors, were co-transfected with the third generation packaging plasmids pMDLg/pRRE,
133 pRSV-Rev, pMSV-VSVG into HEK293T cells using the calcium phosphate transfection method
134 to produce lentiviral particles. The supernatant of HEK293T cells containing virus was
135 harvested at 48 and 72 hours after transfection. Host A549 cells were seeded in six-well
136 plates with a density of 80,000 cells per well and transduced on two consecutive days with
137 the viral supernatant, supplemented with 8 µg/mL polybrene (Sigma-Alrich, Zwijndrecht,
138 Netherlands). The positive transduced cells were selected in 8 µg/mL puromycin
139 supplemented medium for four days from 72h after the last transduction and then were
140 cultured in 1 µg/mL puromycin supplemented medium. Medium was refreshed every 2-3
141 days. Ten days after the last transduction, cells were harvested for western blot, as well as
142 RNA and DNA extraction. In the meantime, cells were grown on coverslips for
143 immunocytochemistry (IHC) and harvested for chromatin immunoprecipitation.

144

145 **Generation of MCF7 stable cell lines**

146 The lentiviral pHAGE-EF1α constructs, encoding the dCas9-SKD and epigenetic editors, were
147 co-transfected with the second generation packaging plasmids psPAX2 and pMD2.G-VSV-G
148 into HEK293T cells using Lipofectamine LTX-PLUS (Life Technologies) to produce lentiviral
149 particles. The supernatant of HEK293T cells containing virus was harvested at 48 and 72
150 hours after transfection. Host MCF7 cells were seeded in six-well plates with a density of

151 80,000 cells per well and transduced on two consecutive days with the viral supernatant,
152 supplemented with 8 µg/mL polybrene (Sigma-Alrich, Zwijndrecht, Netherlands). The
153 positive transduced cells were selected in 8 µg/mL puromycin supplemented medium for
154 four days from 72h after the last transduction and then were cultured in 1 µg/mL puromycin
155 supplemented medium.

156

157 **gRNA Transfections**

158 To transiently transfect the MLM3636 plasmids containing gRNA constructs, 500,000 of each
159 stable MCF7 cells were seeded into 6-well plates the day before transfection. For all
160 experiments, a total of 2 µg of a combination of three gRNA plasmids were cotransfected
161 using 2 µl PLUS reagent and 4 µl Lipofectamine LTX. The cells were then collected two days
162 after transfection to isolate RNA and subcultured for additional 12 days.

163

164 **Detection of mRNA expression by quantitative real-time PCR**

165 Total RNA was extracted from A549 cells using Trizol reagent (Thermo Fisher Scientific) and
166 500 ng was used for cDNA synthesis with random primers using Superscript II RNase H -
167 Reverse transcriptase (Thermo Fisher Scientific). *SPDEF*, *MUC5AC*, *AGR2* and *GAPDH*
168 expression was quantified using qPCR MasterMix Plus (Eurogentec, Belgium) and Taqman
169 gene expression assays (*SPDEF*: Hs01026050_m1; *MUC5AC*: Hs00873651_Mh; *AGR2*:
170 Hs00356521_m1; *GAPDH*: Hs02758991_g1, Thermo Fisher Scientific), mRNA expression of
171 the fusion proteins (FLAG tag), Procollagen-Lysine,2-Oxoglutarate 5-Dioxygenase 2 (*PLOD2*),
172 Tumor Protein P53 (*TP53*), RELA Proto-Oncogene, NF-KB Subunit (*RELA*), Cyclin Dependent
173 Kinase Inhibitor 1A (*CDKN1A*) and beta-actin (*ACTB*) using SYBR® Green PCR Master Mix

174 (Thermo Fisher Scientific) and gene-specific primers (Table 1) with the LightCycler® 480
175 Real-Time PCR System (Roche, Basel, Switzerland). Data were analyzed with LightCycler®
176 480 SW 1.5 software (Roche) and the Fit points method, according to the manufacturer's
177 instructions. Expression levels relative to *GAPDH* were determined with the formula $2^{-\Delta C_p}$
178 (Cp means crossing points).

179

180 **Methylation analysis by pyrosequencing**

181 For DNA methylation analysis of the target regions, genomic DNA was extracted with
182 chloroform-isopropanol and was bisulfite converted using the EZ DNA Methylation-Kit
183 (Zymo Research), following the manufacturer's protocol. Bisulfite-converted DNA was
184 analyzed by pyrosequencing as previously described (7). The primer information for
185 pyrosequencing is presented in Table 1.

186

187 **Histone modification analysis by chromatin immunoprecipitation and qPCR**

188 Histone modification induced by ZFs-G9a was analyzed by ChIP as previously described (12).
189 Briefly, A549 cells were fixed with 1% formaldehyde at 37 °C for 10 min and subsequently
190 lysed and sonicated using a Bioruptor (Diagenode; High, 30 sec on, 30 sec off, total time 15
191 minutes). Sheared chromatin was cleared by centrifuge at 4°C (12,000 × g, 10 minutes). Four
192 microgram of specific antibodies [normal rabbit IgG (abcam, ab46540), H3K9me2 (Milipore,
193 07-441)] were bound to 50 µl of magnetic Dynabeads (Thermo Fisher Scientific) during 15
194 minutes incubation, then unbound antibodies were washed-off. Sheared chromatin 0.25
195 million cells was added to the antibody precoated magnetic Dynabeads (rotating overnight

196 at 4°C). Next day, the magnetic Dynabeads were washed three times with PBS, and
197 chromatin was eluted with 1% (w/v) SDS and 100 mmol/L NaHCO₃. Subsequently, the
198 elutes were treated with RNase (Roche) for four hours and proteinase K (Roche) for one
199 hour at 62°C. Then, the column (Qiagen) purified DNA could be analyzed with quantitative
200 PCR (qPCR).

201 To assess the induction of histone marks and their spreading, several primer pairs were used
202 for the SPDEF promoter (Table 1). qPCR was conducted using SYBR Green PCR Master Mix
203 (Thermo Fisher Scientific) on an LightCycler® 480 Real-Time PCR System (Roche). To
204 calculate the fold induction/reduction of histone marks we used the formula: Percentage
205 input = $2^{(C_{pinput} - C_{pChIP})}$ dilution × factor × 100.

206

207 **Detection of protein expression by western blot**

208 Transduced A549 cells were lysed in RIPA buffer and proteins were analyzed by standard
209 western blotting as previously described (7). Then, the blots were incubated with a rabbit
210 anti-human SPDEF antibody (Santa Cruz, sc-67022), mouse anti-FLAG (Sigma, F3165) and
211 mouse anti-GAPDH (Santa Cruz, sc-47724) at 4°C, overnight, followed by incubation with an
212 horseradish peroxidase (HRP)-conjugated secondary goat anti-rabbit and rabbit anti-mouse
213 antibody (Dako, Glostrup, Denmark). Protein expression was visualized using the Pierce ECL2
214 chemoluminescence detection kit (Thermo Fisher Scientific) and Gel Doc™ XR+ imaging
215 systems (Bio-Rad Laboratories). Data were analyzed with Gel Doc™ XR+ Image Lab™
216 software.

217

218 **Immunocytochemistry**

219 Cells grown on coverslips (Menzel-Gläser, 12 mm in diameter) were washed with PBS and
220 fixed with 2% (w/v) Paraformaldehyde for 20 min. Cells were stained with primary antibody
221 against MUC5AC (Abcam, ab3649), followed by HRP-conjugated secondary antibody. The
222 peroxidase was visualized by staining with AEC (3-amino-9 ethylcarbazole), followed by
223 hematoxylin counterstaining. The cover glasses were mounted with Kaiser's glycerol-gelatin
224 (37°C) and scanned into digital whole slides images using the NanoZoomer series scanning
225 devices. The assessment of immunochemistry staining intensity was performed
226 semiquantitatively in a blinded fashion at four to six of x20 magnification fields. MUC5AC
227 stained cells were categorized as follows: negative (no staining), weak-positive (pink color or
228 small red dot staining) and strong-positive (red staining and >50% of cell volume).

229 FLAG tagged proteins were stained with anti-FLAG antibody (Sigma, F3165), followed by
230 HRP-conjugated secondary antibody and AEC staining. FLAG stained cells were categorized
231 to negative and positive, and counted in a blinded fashion at four x20 magnification fields.

232

233 **Statistics**

234 All transduction experiments were performed at least three times independently. Data were
235 analyzed using one-way ANOVA followed by Bonferroni's Multiple Comparison Test. Data
236 were considered to be statistically significant if $P < 0.05$. Data were expressed as mean \pm SEM
237 and calculated using Prism v5.0 (GraphPad software).

238

239 **Results**

240 ***SPDEF* down regulation by ATFs and subsequent repression of mucus-related genes**

241 To select a suitable model to study *SPDEF* down regulation, *SPDEF* expression was
242 determined in four different human epithelial cell lines: A549, H292, BEAS-2B and 16HBE.
243 A549 cells demonstrated the highest expression of *SPDEF*, both at mRNA level (Fig. 1A) and
244 at protein level (Fig. 1B). The high expression of *SPDEF* in A549 and H292 cells was
245 accompanied by a low degree of DNA methylation at the CpG sites surrounding the
246 transcription start site (TSS) (A549: CpG sites #13: 2.7%, CpG sites #14: 4.6%, CpG sites #15:
247 3.1%; H292: CpG sites #13: 1.9%, CpG sites #14: 4.2%, CpG sites #15: 3.2%), whereas the
248 undetectable transcription levels of *SPDEF* in BEAS-2B and 16HBE were accompanied by a
249 high level of DNA methylation (BEAS-2B: CpG sites #13: 34.9%, CpG sites #14: 40.6%, CpG
250 sites #15: 26.4%; 16HBE: CpG sites #13: 75.9%, CpG sites #14: 68.5%, CpG sites #15: 41.0%)
251 (Fig. 1D). Differential expression of *MUC5AC* was consistent with the observed *SPDEF*
252 expression, with the highest *MUC5AC* expression in A549 cells (Fig. 1C). To explore effective
253 *SPDEF* down regulation, we chose the highest *SPDEF* and *MUC5AC* expressing cell line
254 (A549) as a model.

255 In order to down regulate *SPDEF* expression, four ZFs were designed to bind 18-base pair
256 regions in the *SPDEF* promoter (SPDEF1, SPDEF2, SPDEF3, SPDEF4) and were sub-cloned into
257 lentiviral constructs containing SKD (Fig. 2A). A549 cells were transduced to express the ATF
258 using these lentiviral constructs. To enrich for cells expressing the ATF, the lentiviral
259 transduced cells were positively selected based on puromycin resistance. Correct size of
260 ATFs was confirmed by western blot (Fig. 2C) and their nuclear location by
261 immunohistochemical staining (Fig. 3D). FLAG positive cells ranged from 15% (SKD-SPDEF2)

262 to 64% (SKD-SPDEF3) after the selection with puromycin (Fig 3D). According to the FLAG
263 staining, SKD-SPDEF1 was expressed to a similar degree as SKD-SPDEF2, and both were
264 generally lower expressed than SKD-SPDEF3 and SKD-SPDEF4.

265

266 Next, we examined the ability of the four ATFs to down regulate *SPDEF* mRNA expression in
267 A549 cells. As shown in Fig. 2B, all four ATFs significantly down regulated *SPDEF* expression,
268 demonstrating 70, 97, 93, and 96% respectively down regulation relative to empty vector
269 control, which was confirmed at the protein level (Fig. 2C).

270 As *SPDEF* regulates a network of genes associated with mucus production (2, 20, 28), we
271 investigated whether the down regulation of *SPDEF* expression mediated by ATFs indeed
272 resulted in reduced expression of mucus-related genes. Therefore, the expression level of
273 two downstream mucus-related genes was investigated in the ATF-expressing A549 cells.

274 We found that expression of *AGR2* was significantly down regulated by SKD-SPDEF2
275 (90.9%±35.4% repression), SKD-SPDEF3 (79.3%±35.9% repression) and SKD-SPDEF4
276 (86.2%±35.4% repression) (Fig. 3A). *MUC5AC* was consistently, yet not significantly, down
277 regulated in response to *SPDEF* repression (Fig. 3B). However, MUC5AC immunohistochemistry
278 staining on ATF-transduced A549 cells supports successful inhibition at the protein level (Fig.
279 3C and 3D).

280 ***SPDEF* silencing by targeted epigenetic editing**

281 In order to achieve the stable gene silencing, we set out to direct DNA methylation onto the
282 *SPDEF* promoter. As DNA methylation levels of CpG sites #13 (-3 bp), #14 (-1 bp) and #15
283 (+40 bp) around the TSS negatively correlated with *SPDEF* expression, ZF SPDEF3 targeting
284 location -131 to -114 bp was coupled to the catalytic domain of DNMT3A. To investigate the

285 induced DNA methylation in the promoter region of *SPDEF*, 15 CpG sites were screened with
286 pyrosequencing (Fig. 4). We found that DNA methylation was induced on CpGs sites #14 and
287 15, and not on CpG sites #1-13. In further experiments, CpG sites #13-15 were analyzed.
288 SPDEF3-DNMT3A consistently deposited DNA methylation onto two CpG sites (CpG #14: 6.6
289 \pm 0.8%; CpG #15: 10.5 \pm 1.3%), compared with SPDEF3-NOED (CpG #site 14: 3.9 \pm 0.3%; CpG
290 #15: 5.2 \pm 0.8%) (Fig. 5B). To determine whether the observed increase in DNA methylation
291 was directly caused by the catalytic activity of the DNMT3A enzyme, a catalytic mutant of
292 DNMT3A (DNMT3A E74A) was constructed and compared to DNMT3A in a separate set of
293 experiments. No increase in DNA methylation was observed for CpG sites #13-15 in SPDEF3-
294 DNMT3A E74A treated cells (Fig. 5C). To investigate whether the ZF directed DNMT3A was
295 able to reduce target gene transcription, *SPDEF* mRNA expression was investigated (Fig. 6A,
296 left panel). SPDEF3-DNMT3A was able to down regulate *SPDEF* expression (76.6% \pm 25.5%
297 repression), which was equally efficient as repression induced by the positive control SKD-
298 SPDEF3 (79.1% \pm 12.7% repression). Interestingly, the construct that lacked the effector
299 domain, SPDEF3-NOED, also reduced *SPDEF* expression significantly (72.0% \pm 25.3%
300 repression). To determine the influence of location, another ZF (SPDEF4: target sequence
301 +112 to +129) was tested to target DNMT3A to the *SPDEF* promoter. We found that SPDEF4-
302 DNMT3A was able to better down regulate *SPDEF* expression (86.9% \pm 12.1% repression)
303 than control SPDEF4-NOED (46.8% \pm 35.1% *SPDEF* repression) and the catalytic mutant (Fig.
304 6A), even though SPDEF4-DNMT3A didn't induce methylation changes in the investigated
305 region CpG13-15 (Fig. 5D).

306 Upon ZFs fused with the histone methyltransferase G9A, again, SPDEF4-G9A was able to
307 down regulate *SPDEF* expression equally efficiently as positive control SKD-SPDEF4 and
308 further repressed *SPDEF* expression than SPDEF4-NOED (Fig. 6A) However, no difference

309 was detected between SPDEF4-G9A and its mutant and no H3K9me2 marks were detected
310 in the examined region (data not shown). The expression of the fusion proteins was
311 confirmed by the mRNA expression of the FLAG-tag (Fig. 7). The SPDEF4-DNMT3A construct
312 was not higher expressed than its mutant, indicating that enhanced *SPDEF* repression of
313 SPDEF4-DNMT3A compared to its mutant was not because of more occupation of ZFs
314 SPDEF4 itself.

315 Down regulation of *SPDEF* by SPDEF3-DNMT3A, SPDEF4-DNMT3A, SPDEF3-G9A and SPDEF4-
316 G9A was confirmed at the protein level by western blot (Fig. 8). Importantly, expression of
317 downstream mucus related genes *AGR2* and *MUC5AC* was also down regulated by these
318 constructs (Fig. 6B and 6C).

319 **Lower number of strong MUC5AC positive cells after targeted silencing *SPDEF* by**
320 **epigenetic editing**

321 The effect of *SPDEF* inhibition on mucus production was determined by quantification of the
322 number of MUC5AC positive cells. Transduced A549 cells were seeded on cover slips and
323 examined by immunocytochemistry staining. Interestingly, *SPDEF* silencing was most effective
324 within the MUC5AC strong positive cell population. Within this population, both SPDEF3-
325 DNMT3A and SPDEF4-G9a treatment resulted in lower numbers of MUC5AC strong positive
326 (Fig. 9B). To rule out that the effects were caused by a general repressive effect of either
327 G9A or DNMT3A, we determined expression levels of four irrelevant genes (*PLOD2*, *TP53*,
328 *RELA* and *CDKN1A*) and found that none of these demonstrated inhibition of expression (Fig.
329 10).

330

331 **Sustained epigenetic repression of *SPDEF* by epigenetic editing**

332 To further address the effectiveness and sustainability of gene repression by epigenetic
333 editing, we decided to use the CRISPR-dCas9 system. We engineered stable MCF7 cell lines,
334 each one expressing dCas9 fusions either with the transcriptional repressor SKD, several
335 epigenetic editors or their mutants (G9a and SUV39h1 (for H3K9me), the SET domain of
336 EZH2 (for H3K27me), or a chimeric DNMT3a-DNMT3L fusion (for DNA methylation(30))). We
337 designed three gRNAs to bind around the promoter of *SPDEF*. By transiently transfecting a
338 mix of the three gRNAs into the stable cell lines, we were able to address the maintenance
339 of gene repression (Fig. 11A). Gene repression was achieved to similar degrees two days
340 after transfecting the mix of gRNAs in all stable cell lines. As observed for ZF-fusions,
341 repression was also observed when using the mutant effector domains (Figs. 11 B-E).
342 Importantly, for several other genes no such repressive effects by dCas9 without effector
343 domain have been observed in this stable system (data not shown). While repression by the
344 transcriptional repressor SKD and most of the epigenetic editors was not maintained, the
345 repression of *SPDEF* was sustained when using the G9a effector domain, while the mutant
346 fusion regained activation.

347 **Discussion**

348 Based on its important role in goblet cell differentiation and mucus production (6, 26), we
349 reasoned that *SPDEF* could be a suitable therapeutic target against mucus hypersecretion. In
350 this study, we were able to silence *SPDEF* expression in the human alveolar epithelial cell
351 line A549, using a novel strategy: engineered *SPDEF* targeting ZF proteins directing
352 transcriptional repressor (SKD), as well as epigenetic enzymes (DNMT3A and G9A). The

353 repression of *SPDEF* was accompanied by lower expression of mucus-related genes *MUC5AC*
354 and *AGR2*, as well as lower numbers of MUC5AC positive cells.

355 Our data provides an original proof-of-concept study supporting *SPDEF* as a promising
356 therapeutic target for inhibiting mucus production, which is amenable to stable repression
357 with epigenetic editing. As previously reported, knockdown of *SPDEF* using siRNA was able
358 to reduce the IL-13-induced expression of MUC5AC and AGR2 in human airway epithelial
359 16HBE cells (36). The principle of siRNA is to target and degrade mRNA. Because of the
360 constant production of mRNA, the silencing effect of siRNA is generally transient and it has
361 to be delivered repeatedly in clinical application. Epigenetic editing would be a superior
362 strategy because the effect would be sustained after clearance of the drug (hit and run
363 approach) (8). In order to down-regulate *SPDEF* expression directly at the transcriptional
364 level, four sequence-specific ZFs were generated. ZFs were first linked to SKD to test the
365 functionality of the DNA binding domain because SKD can cause transient gene silencing by
366 indirectly recruiting chromatin remodelers and histone-modifying enzymes (28, 32). These
367 four ATFs (ZF-SKD) strongly reduced *SPDEF* expression and nearly abolished all expression of
368 *SPDEF* in A549 cells. More importantly, *SPDEF* silencing resulted in the additional down
369 regulation of MUC5AC mRNA and protein expression as well, indicating successful inhibition
370 of mucin synthesis.

371 Next, ZFs were fused to catalytic domains of epigenetic enzymes (DNMT3A and G9A), aiming
372 for longer term gene silencing by changing the epigenetic state of the targeted gene. ZF-
373 targeted DNA methylation was recently successfully used for silencing several cancer-
374 associated genes, including VEGF-A, SOXA2, and EpCAM (24, 28, 29, 31). Here, we took
375 advantage of this approach by using two different ZFs engineered close to the TSS (*SPDEF3*

376 and SPDEF4), to down regulate *SPDEF* expression. In this area, high expression of *SPDEF* was
377 accompanied by lower DNA methylation of CpG sites, particularly those surrounding the
378 TSS, where DNA methylation is tightly linked to transcriptional silencing (3). The occlusion
379 binding of TF also explains our observation that ZFs without effector domains effectively
380 silenced *SPDEF* expression. We observed similar strong *SPDEF* repressive effects upon
381 targeting ZFs without any effector domain as upon targeting ZFs fused with repressor SKDs.
382 Many factors can explain the repressive effects of the binding of the gene targeting
383 constructs, like competition with endogenous transcription factors, such as SMAD, or
384 components of the preinitiation complex formation. Importantly, the effects were also
385 obtained when targeting CRISPR-dCas9 without an effector by the sgRNAs (20), indicating
386 that steric hindrance might indeed explain the repressive effect. Since such effects generally
387 are transient, it is important to assess that addition of domains to the targeting moiety do
388 not affect inhibition properties. Importantly, the fusion of effector domains to the ZFs did
389 not hamper the repressive effect of the ZF approach.

390 As the DNA binding domain by itself, or in fusion with SKD, is not expected to induce any
391 long-term effects, we next set out to test different epigenetic enzymes (DNMT3A and G9A).
392 Fusion of epigenetic effector domains with ZFs resulted in the same magnitude of silencing
393 as the ZF-SKD fusions, indicating that our approach worked as we aimed for. Furthermore,
394 targeted DNA methylation or histone methylation has the advantage that its effect has the
395 potential to be permanent (4, 28, 31), albeit the stability and heritability of epigenetic
396 editing is still controversial (14, 19) and likely depend on the local chromatin modification
397 state (4).

398 In an elegant experiment, Bintu and colleagues used an artificial system to compare four
399 repressive chromatin regulators with distinct chromatin modifications (2): the embryonic
400 ectoderm development (EED) protein of Polycomb repressive complex 2, which indirectly
401 catalyzes H3K27 methylation, the KRAB domain, that indirectly promotes H3K9 methylation,
402 the DNMT3B, that catalyzes DNA methylation and the histone deacetylase 4 (HDAC4)
403 enzyme. By transiently recruiting each protein, they demonstrate that different types of
404 repressed chromatin are generally associated with distinct time scales of repression. For this
405 artificial context, DNA methylation was the modification of choice to achieve long lasting
406 repression, while histone deacetylation was not sustained. Only few studies so far have
407 addressed stable silencing of endogenous genes, and controversial effects have been
408 reported (1, 19, 31). Here, we provide indications that targeting epigenetic effector domains
409 to *SPDEF* has the ability to promote sustained gene expression reprogramming. Indeed, we
410 demonstrated that upon targeting G9A, maintenance of repression was obtained, which
411 was not observed for the transcriptional repressor SKD, DNA methyltransferase or other
412 histone modifiers. These differences in maintenance require more thorough investigations,
413 but likely are due to the particular local chromatin context of the targeted locus, that could
414 influence the potency and longevity of epigenetic reprogramming. This would also explain
415 the reported failure of maintenance of induced H3K9methylation effects when studying
416 VEGF-A repression (19). Combining different effector domains, as we did previously for re-
417 activation of gene expression, might further improve the degree of repression and/or
418 increase sustainability (4). Indeed, Amabile et al recently demonstrated the importance of
419 co-targeting KRAB, DNMT3A and DNMT3L in inducing maintained repression for
420 endogenous genes (1).

421 One limitation of our study is that functional experiments were conducted in the alveolar
422 cell line A549. Since we already showed convincing *MUC5AC* and *AGR2* silencing in A549
423 cells, it will be interesting to investigate whether this effect is also observed within the more
424 relevant models of mucus hypersecretion in the future, such as using the air-liquid interface
425 culture of the primary airway epithelial cells from patients with COPD. In addition, before
426 use in the clinical setting, it is necessary to further evaluate the off-target effects, such as
427 the ZFs or CRISPR/dCas9 binding specificity and target cell specificity.

428 In summary, we successfully reduced mucus-related gene expression by targeted silencing
429 of *SPDEF*. This new approach (epigenetic editing) has the potential to induce a permanent
430 anti-mucus effect, which has implications for development of novel therapeutic strategies to
431 treat patients with chronic mucus hypersecretion in the future.

432

433 **Acknowledgements**

434 The authors would like to thank, JM Dokter-Fokkens, PG Jellema, MGP van der Wijst, and K
435 Meyer, Department of Pathology and Medical Biology, University Medical Center Groningen
436 (UMCG), for technical help with this study.

437 **Support statement:** This work was supported by grants from the Stichting Astma Bestrijding
438 (project 2014/007) and the Jan Kornelis de Cock Stichting (project 2014-62). JS is supported
439 by the Abel Tasman Talent Program, University Medical Center Groningen. DCR is supported
440 by Samenwerkingsverband Noord-Nederland SNN-4D22C-T2007. DG is supported by EU
441 funding H2020-MSCA-ITN-2014-ETN 642691 EpiPredict. TPJ is supported by Baden-
442 Württemberg Stiftung (95011370). MH is MC member of COST (Cooperation in Science and
443 Technology) Action BM1201. MGR is vice-chair of COST Action CM 1406 (EpiChemBio.eu).

444 Conflict of interest: None declared.

445

446

447

448 Table 1 PCR and sequencing primers

Primer Name	Sequence (5'- 3')	Application
SPDEF Pyro-A F	GGGTTATGGGAGAGTAAGTTGT	PCR and sequencing for SPDEF-A pyrosequencing
SPDEF Pyro-A R	[Biotin]TCTATACCCACAAAATCCTCAT	
SPDEF Pyro-A Seq	GTTGTTGGTTGGTTT	
SPDEF Pyro-B/C F	GGATTTTGTGGGGTATAGAGAA	PCR and sequencing for SPDEF-B/C pyrosequencing
SPDEF Pyro-B/C R	[Biotin]ATTACTACATAACCACTCAACTCATATT	
SPDEF Pyro-B Seq	GGGGTATAGAGAATATAGTT	
SPDEF Pyro-C Seq	TTTAGAATTTTAGTTTTGGATTTA	
SPDEF Pyro-D/E F	ATGAGTTGAGTGGTTATGTAGTAAT	PCR and sequencing for SPDEF-D/E pyrosequencing
SPDEF Pyro-D/E R	[Biotin]CCAACCCAAAACCTACTACTAAC	
SPDEF Pyro-D Seq	AGTGGTTATGTAGTAATTAATG	
SPDEF Pyro-E Seq	AATTAGGTTTTGGTTAATTT	
DNMT3a-E74A F	CATTGCCTCCGCCGTGTGTGAGG	PCR for DNMT3a-E74A site mutagenesis
DNMT3a-E74A R	TAGCGGTCCACTTGGATGC	
NOED F	CGCGCCATGCATGATCATTTAAATTTAAT	PCR for NOED cloning
NOED R	TAAATTTAAATGATCATGCATGG	
SPDEF-ChIP-region 1 F	GCATGGGTGGTTCTGGATCT	ChIP-qRT-PCR for SPDEF region 1
SPDEF-ChIP-region 1 R	GCCAGAGATACGTCGAGTGG	
SPDEF-ChIP-region 2 F	GCAGCAACCAATGAACGAGTG	ChIP-qRT-PCR for SPDEF region 2
SPDEF-ChIP-region 2 R	ATTAACCTTGCAGGTCTCCC	

SPDEF-ChIP-region 3 F	CCAGCACATTCCTGCACTCT	ChIP-qRT-PCR for SPDEF region 3
SPDEF-ChIP-region 3 R	CAACCTGAGGGGCTTGCAAG	
FLAG-F	TGAATCGGTAGGAATTCGCGG	qRT-PCR for <i>FLAG</i>
FLAG-R	GGGAGGGGCAAACAACAGAT	
GAPDH-F	CCACATCGCTCAGACACCAT	qRT-PCR for <i>GAPDH</i>
GAPDH-R	GCGCCCAATACGACCAAAT	
ACTB-F	CCAACCGCGAGAAGATGA	qRT-PCR for <i>ACTB</i>
ACTB-R	CCAGAGGCGTACAGGGATAG	
RELA-F	CGGGATGGCTTCTATGAGG	qRT-PCR for <i>RELA</i>
RELA-R	CTCCAGGTCCCGCTTCTT	
TP53-F	GCTCAAGACTGGCGCTAAAA	qRT-PCR for <i>TP53</i>
TP53-R	GTCACCGTCGTGGAAAGC	
PLOD2-F	GGGAGTTCATTGCACCAGTT	qRT-PCR for <i>PLOD2</i>
PLOD2-R	GAGGACGAAGAGAACGC	
CDKN1A-F	TCACTGTCTTGTACCCTTGTGC	qRT-PCR for <i>CDKN1A</i>
CDKN1A-R	GGCGTTTGGAGTGGTAGAAA	

449

450

451 **Figure legends**

452 **Figure 1** Expression of *SPDEF* (mRNA and protein) is associated with DNA methylation and
453 *MUC5AC* expression. Quantification of the mRNA levels of *SPDEF* (A) and *MUC5AC* (C) in a
454 panel of human epithelial cell lines (A549, H292, BEAS-2B, and 16HBE) by qRT-PCR. Dot plots
455 represent the mean and variation of three independent experiments. (B) Visualization of
456 *SPDEF* protein expression (left) and quantification relative to β -ACTIN (right), as conducted
457 by western blot (n=1). An anti- β -ACTIN antibody was used as a loading control. (D)
458 Quantitative analysis of the methylation levels of three CpG sites surrounding transcription
459 start site (TSS) by pyrosequencing. Scatter plots show two independent experiments.

460 **Figure 2** *SPDEF*-targeted silencing by ATFs in A549 cells. (A) Schematic representations of
461 the promoter region of the *SPDEF* gene, outlining the putative binding sites for transcription
462 factors (STAT6, NKX2-1/NKX3-1, GFI, FOXA1/FOXA2, SMAD) (MatInspector) and the target
463 sequences of zinc fingers: SPDEF1, SPDEF2, SPDEF3, and SPDEF4. Arrows show the
464 orientation of the 18-bp binding site in the promoter. Location of ZF was shown relative to
465 the TSS (+1). The translation start site was shown as ATG (+286). CpGs are indicated as
466 vertical bars. DNA methylation status of 15 CpGs was analyzed using pyrosequencing for the
467 indicated areas. Histone modification of H3K9me2 was assessed for the CHIP regions (gray
468 boxes). (B) Relative *SPDEF* mRNA expression, normalized to the empty vector, assessed by
469 quantitative RT-PCR in transduced A549 cells. Data are presented as mean and variation of
470 three independent experiments. Statistical significance was analyzed using one-way ANOVA
471 followed by Bonferroni's Multiple Comparison Test (*P<0.05, **P<0.01). (C) *SPDEF* protein
472 expression in transduced A549 cells, as conducted by western blot. An anti- Glyceraldehyde
473 3-phosphate dehydrogenase (GAPDH) antibody was used as a loading control. An anti-FLAG

474 antibody was used to detect the ATFs, which were designed with a C-terminal 3×FLAG tag.

475 Blot pictures shown are representative of two independent experiments.

476 **Figure 3** Changes in downstream mucus-related genes after ATFs induced silencing of

477 *SPDEF*. (A) *MUC5AC* and (B) *AGR2* mRNA expression were investigated by quantitative RT-

478 PCR. Data are presented as mean and variation of three independent experiments.

479 Statistical significance was analyzed using one-way ANOVA followed by Bonferroni's

480 Multiple Comparison Test (* $P < 0.05$, ** $P < 0.01$). (C) Quantification of *MUC5AC* negative,

481 weak- and strong-positive A549 cells after ATF treatment. Counting of cells was performed

482 in a blinded fashion. Solid bars, strong positive; shaded bars, weak positive; open bars,

483 negative. Results represent the average of two independent experiments. (D)

484 Representative photographs (original magnification, ×20) from immunocytochemistry staining

485 for *MUC5AC* (upper panel) and FLAG (lower panel) in ATFs treated A549 cells. Red-stained

486 cells are *MUC5AC*-positive and FLAG-positive respectively. Nuclei were counterstained with

487 hematoxylin. Scale bar: 100 μm .

488 **Figure 4** Screening of the DNA methylation changes after targeting DNMT3A to *SPDEF*

489 promoter. Quantitative analysis is the percentage of methylation for 14 CpG sites in *SPDEF*

490 promoter by pyrosequencing in A549 cells treated with mock, empty vector, *SPDEF3*-NOED

491 and *SPDEF3*-DNMT3A in one experiment. (A) CpG sites #1, #3, and #4; (B) CpG sites #5-8; (C)

492 CpG sites #9-12; (D) CpG sites #13-15.

493 **Figure 5** DNA methylation changes after targeting DNMT3A to *SPDEF* promoter. (A)

494 Schematic presentation of *SPDEF3*-DNMT3A and *SPDEF4*-DNMT3A, and their binding

495 location relative to TSS. (B) Quantitative analysis the percentage of methylation for target

496 CpG sites (#13, #14 and #15) by pyrosequencing in A549 cells treated with mock, empty

497 vector, *SPDEF3*-NOED and *SPDEF3*-DNMT3A (n=4). (C) Relative DNA methylation level of

498 A549 cells after treatment with SPDEF3-NOED, SPDEF3-DNMT3A and SPDEF3-DNMT3A E74A
499 normalized to SPDEF3-NOED (n=3). (D) Relative DNA methylation level of A549 cells after
500 treatment with SPDEF4-NOED, SPDEF4-DNMT3A and SPDEF4-DNMT3A E74A normalized to
501 SPDEF4-NOED (n=3). Dot plots represent the mean and variation of at least three
502 independent experiments. Statistical significance was analyzed using one-way ANOVA
503 followed by Bonferroni's Multiple Comparison Test (*P<0.05, compared to empty vector;
504 #P<0.05, ##P<0.01, compared between two indicated columns).

505 **Figure 6** *SPDEF* and downstream mucus related genes expression changes after targeting
506 DNMT3A and G9a to *SPDEF* promoter. A549 cells were treated with ZFs fused with different
507 effector domains (SKD, DNMT3A, G9a, and the respective mutants DNMT3A E74A and G9a
508 W1050A). mRNA level of (A) *SPDEF*, (B) *AGR2* and (C) *MUC5AC* were determined by
509 quantitative RT-PCR on treated A549 cells. The expression of *SPDEF* was relative to *GAPDH*
510 and normalized to mock treated cells (left panel), or normalized to ZF-NOED (middle and
511 right panels) to enlarge any difference between wild type and mutant effectors. Dot plots
512 represent the mean and variation of at least three independent experiments. Statistical
513 significance was analyzed using one-way ANOVA followed by Bonferroni's Multiple
514 Comparison Test (*P<0.05, **P<0.01, ***P<0.001, compared to empty vector; #P<0.05,
515 ##P<0.01, ###P<0.001, compared between two indicated columns).

516 **Figure 7** Expression of ZF-ED after A549 cells treated with ZF fused to different effector
517 domain (SKD, DNMT3A, G9a, and respective mutant DNMT3A E74A and G9a W1050A). The
518 expression of ZF-ED was represented as the FLAG-tag expression relative to *GAPDH* (A), and
519 normalized to ZF-NOED (B and C). Dot plots represent the mean and variation of three
520 independent experiments. Statistical significance was analyzed using one-way ANOVA

521 followed by Bonferroni's Multiple Comparison Test (#P<0.05, ##P<0.01, ###P<0.001,
522 compared between two indicated columns).

523 **Figure 8** Quantification of the changes of SPDEF protein levels in A549 cells treated with
524 *SPDEF* targeted DNMT3A and G9a. A549 cells were treated with ZF fused with different
525 effector domains (SKD, DNMT3A, G9a, and respective mutant DNMT3A E74A and G9a
526 W1050A). (A) Protein expression of SPDEF was assessed by Western blot. An anti-GAPDH
527 antibody was used as a loading control. Blot pictures shown are representative of three
528 independent experiments. (B) Densitometric values of SPDEF were normalized against the
529 loading control, GAPDH. The relative level (ratio to mock) of SPDEF was shown with the
530 average of three independent experiments. Statistical significance was analyzed using one-
531 way ANOVA followed by Bonferroni's Multiple Comparison Test (*P<0.05, **P<0.01,
532 compared to empty vector).

533 **Figure 9** Quantification of MUC5AC positive A549 cells after treatment with *SPDEF* targeted
534 DNMT3A and G9a. A549 cells were treated with ZFs fused with different effector domains
535 (SKD, DNMT3A, G9a, and respective mutant DNMT3A E74A and G9a W1050A) and grown on
536 coverslips. Immunocytochemistry staining for MUC5AC was quantified to negative, weak-
537 positive and strong-positive in a blinded fashion. (A) Percentage of MUC5AC positive cells in
538 the total cell populations. (B) Percentage of MUC5AC strong-positive cells in the total cell
539 populations. Results are represented as mean and variation of three independent
540 experiments. Statistical significance was analyzed using one-way ANOVA followed by
541 Bonferroni's Multiple Comparison Test (*P<0.05, compared to empty vector).

542 **Figure 10** Expression of irrelevant genes after A549 cells treated with ZF fused to different
543 effector domain (DNMT3A, G9a, and respective mutant DNMT3A E74A and G9a W1050A).

544 The expression of *PLOD2* (A), *TP53* (B), *RELA* (C) and *CDKN1A* (D) was relative to *ACTB*. The
545 dot plots represent the mean and variation of three independent experiments.

546 **Figure 11** Sustained gene repression by means of epigenetic editing using the CRISPR-dCas9
547 system. (A) Schematic representation of the experimental setup with the stable MCF7 cells.
548 mRNA level of *SPDEF* determined by quantitative RT-PCR on MCF7 stable cells with dCas9-
549 (B) SKD, (C) G9a and its mutant and Suv39h1 (D) SET and its mutant and (E) DNMT3a3L and
550 its mutant. Results are represented as average (\pm SEM) of three independent experiments.

551

552 **References**

- 553 1. **Amabile A, Migliara A, Capasso P, Biffi M, Cittaro D, Naldini L, and Lombardo**
554 **A.** Inheritable Silencing of Endogenous Genes by Hit-and-Run Targeted Epigenetic Editing.
555 *Cell* 167: 219-232 e214, 2016.
- 556 2. **Bintu L, Yong J, Antebi YE, McCue K, Kazuki Y, Uno N, Oshimura M, and**
557 **Elowitz MB.** Dynamics of epigenetic regulation at the single-cell level. *Science* 351: 720-
558 724, 2016.
- 559 3. **Brenet F, Moh M, Funk P, Feierstein E, Viale AJ, Socci ND, and Scandura JM.**
560 DNA methylation of the first exon is tightly linked to transcriptional silencing. *PloS one* 6:
561 e14524, 2011.
- 562 4. **Cano-Rodriguez D, Gjaltema RA, Jilderda LJ, Jellema P, Dokter-Fokkens J,**
563 **Ruiters MH, and Rots MG.** Writing of H3K4Me3 overcomes epigenetic silencing in a
564 sustained but context-dependent manner. *Nature communications* 7: 12284, 2016.
- 565 5. **Cano-Rodriguez D, and Rots MG.** Epigenetic Editing: On the Verge of
566 Reprogramming Gene Expression at Will. *Current Genetic Medicine Reports* 1-10, 2016.
- 567 6. **Chen G, Korfhagen TR, Xu Y, Kitzmiller J, Wert SE, Maeda Y, Gregorieff A,**
568 **Clevers H, and Whitsett JA.** SPDEF is required for mouse pulmonary goblet cell
569 differentiation and regulates a network of genes associated with mucus production. *Journal of*
570 *Clinical Investigation* 119: 2914-2924, 2009.
- 571 7. **Chen H, Kazemier HG, de Groote ML, Ruiters MH, Xu GL, and Rots MG.**
572 Induced DNA demethylation by targeting Ten-Eleven Translocation 2 to the human ICAM-1
573 promoter. *Nucleic acids research* 42: 1563-1574, 2014.
- 574 8. **de Groote ML, Verschure PJ, and Rots MG.** Epigenetic Editing: targeted rewriting
575 of epigenetic marks to modulate expression of selected target genes. *Nucleic acids research*
576 40: 10596-10613, 2012.
- 577 9. **Fahy JV, and Dickey BF.** Airway mucus function and dysfunction. *The New*
578 *England journal of medicine* 363: 2233-2247, 2010.
- 579 10. **Falahi F, Huisman C, Kazemier HG, van der Vlies P, Kok K, Hospers GA, and**
580 **Rots MG.** Towards sustained silencing of HER2/neu in cancer by epigenetic editing.
581 *Molecular cancer research : MCR* 11: 1029-1039, 2013.
- 582 11. **Gao W, Li L, Wang Y, Zhang S, Adcock IM, Barnes PJ, Huang M, and Yao X.**
583 Bronchial epithelial cells: The key effector cells in the pathogenesis of chronic obstructive
584 pulmonary disease? *Respirology* 20: 722-729, 2015.
- 585 12. **Gjaltema RAF, de Rond S, Rots MG, and Bank RA.** Procollagen Lysyl
586 Hydroxylase 2 Expression Is Regulated by an Alternative Downstream Transforming Growth
587 Factor beta-1 Activation Mechanism. *Journal of Biological Chemistry* 290: 28465-28476,
588 2015.
- 589 13. **Gowher H, Loutchanwoot P, Vorobjeva O, Handa V, Jurkowska RZ, Jurkowski**
590 **TP, and Jeltsch A.** Mutational analysis of the catalytic domain of the murine Dnmt3a DNA-
591 (cytosine C5)-methyltransferase. *Journal of molecular biology* 357: 928-941, 2006.
- 592 14. **Hathaway NA, Bell O, Hodges C, Miller EL, Neel DS, and Crabtree GR.**
593 Dynamics and memory of heterochromatin in living cells. *Cell* 149: 1447-1460, 2012.
- 594 15. **Heijink IH, Brandenburg SM, Noordhoek JA, Postma DS, Slebos D-J, and van**
595 **Oosterhout AJM.** Characterisation of cell adhesion in airway epithelial cell types using
596 electric cell-substrate impedance sensing. *European Respiratory Journal* 35: 894-903, 2010.
- 597 16. **Huisman C, Wisman GB, Kazemier HG, van Vugt MA, van der Zee AG,**
598 **Schuuring E, and Rots MG.** Functional validation of putative tumor suppressor gene

599 C13ORF18 in cervical cancer by Artificial Transcription Factors. *Molecular oncology* 7: 669-
600 679, 2013.

601 17. **Jurkowski TP, Ravichandran M, and Stepper P.** Synthetic epigenetics—towards
602 intelligent control of epigenetic states and cell identity. *Clinical epigenetics* 7: 18, 2015.

603 18. **Kearns NA, Genga RM, Enameh MS, Garber M, Wolfe SA, and Maehr R.** Cas9
604 effector-mediated regulation of transcription and differentiation in human pluripotent stem
605 cells. *Development* 141: 219-223, 2014.

606 19. **Kungulovski G, Nunna S, Thomas M, Zanger UM, Reinhardt R, and Jeltsch A.**
607 Targeted epigenome editing of an endogenous locus with chromatin modifiers is not stably
608 maintained. *Epigenetics & chromatin* 8: 12, 2015.

609 20. **Larson MH, Gilbert LA, Wang X, Lim WA, Weissman JS, and Qi LS.** CRISPR
610 interference (CRISPRi) for sequence-specific control of gene expression. *Nat Protoc* 8: 2180-
611 2196, 2013.

612 21. **Martin C, Frija-Masson J, and Burgel PR.** Targeting mucus hypersecretion: new
613 therapeutic opportunities for COPD? *Drugs* 74: 1073-1089, 2014.

614 22. **McCauley HA, and Guasch G.** Three cheers for the goblet cell: maintaining
615 homeostasis in mucosal epithelia. *Trends in molecular medicine* 21: 492-503, 2015.

616 23. **Miravittles M.** Cough and sputum production as risk factors for poor outcomes in
617 patients with COPD. *Resp Med* 105: 1118-1128, 2011.

618 24. **Nunna S, Reinhardt R, Ragozin S, and Jeltsch A.** Targeted methylation of the
619 epithelial cell adhesion molecule (EpCAM) promoter to silence its expression in ovarian
620 cancer cells. *PloS one* 9: e87703, 2014.

621 25. **Park KS, Korfhagen TR, Bruno MD, Kitzmiller JA, Wan H, Wert SE, Khurana**
622 **Hershey GK, Chen G, and Whitsett JA.** SPDEF regulates goblet cell hyperplasia in the
623 airway epithelium. *J Clin Invest* 117: 978-988, 2007.

624 26. **Rajavelu P, Chen G, Xu Y, Kitzmiller JA, Korfhagen TR, and Whitsett JA.**
625 Airway epithelial SPDEF integrates goblet cell differentiation and pulmonary Th2
626 inflammation. *J Clin Invest* 125: 2021-2031, 2015.

627 27. **Ramos FL, Krahnke JS, and Kim V.** Clinical issues of mucus accumulation in
628 COPD. *International journal of chronic obstructive pulmonary disease* 9: 139-150, 2014.

629 28. **Rivenbark AG, Stolzenburg S, Beltran AS, Yuan X, Rots MG, Strahl BD, and**
630 **Blancafort P.** Epigenetic reprogramming of cancer cells via targeted DNA methylation.
631 *Epigenetics* 7: 350-360, 2012.

632 29. **Siddique AN, Nunna S, Rajavelu A, Zhang Y, Jurkowska RZ, Reinhardt R, Rots**
633 **MG, Ragozin S, Jurkowski TP, and Jeltsch A.** Targeted methylation and gene silencing of
634 VEGF-A in human cells by using a designed Dnmt3a-Dnmt3L single-chain fusion protein
635 with increased DNA methylation activity. *Journal of molecular biology* 425: 479-491, 2013.

636 30. **Stepper P, Kungulovski G, Jurkowska RZ, Chandra T, Krueger F, Reinhardt R,**
637 **Reik W, Jeltsch A, and Jurkowski TP.** Efficient targeted DNA methylation with chimeric
638 dCas9-Dnmt3a-Dnmt3L methyltransferase. *Nucleic acids research* 2016.

639 31. **Stolzenburg S, Beltran AS, Swift-Scanlan T, Rivenbark AG, Rashwan R, and**
640 **Blancafort P.** Stable oncogenic silencing in vivo by programmable and targeted de novo
641 DNA methylation in breast cancer. *Oncogene* 34: 5427-5435, 2015.

642 32. **Stolzenburg S, Rots MG, Beltran AS, Rivenbark AG, Yuan X, Qian H, Strahl**
643 **BD, and Blancafort P.** Targeted silencing of the oncogenic transcription factor SOX2 in
644 breast cancer. *Nucleic acids research* 40: 6725-6740, 2012.

645 33. **Thakore PI, Black JB, Hilton IB, and Gersbach CA.** Editing the epigenome:
646 technologies for programmable transcription and epigenetic modulation. *Nature methods* 13:
647 127-137, 2016.

- 648 34. **Thomson NC, Chaudhuri R, Messow CM, Spears M, MacNee W, Connell M,**
649 **Murchison JT, Sproule M, and McSharry C.** Chronic cough and sputum production are
650 associated with worse clinical outcomes in stable asthma. *Respir Med* 107: 1501-1508, 2013.
- 651 35. **Wang G, Xu Z, Wang R, Al-Hijji M, Salit J, Strulovici-Barel Y, Tilley AE,**
652 **Mezey JG, and Crystal RG.** Genes associated with MUC5AC expression in small airway
653 epithelium of human smokers and non-smokers. *BMC medical genomics* 5: 21, 2012.
- 654 36. **Yu H, Li Q, Kolosov VP, Perelman JM, and Zhou X.** Interleukin-13 induces mucin
655 5AC production involving STAT6/SPDEF in human airway epithelial cells. *Cell*
656 *communication & adhesion* 17: 83-92, 2010.

657

Figure 1

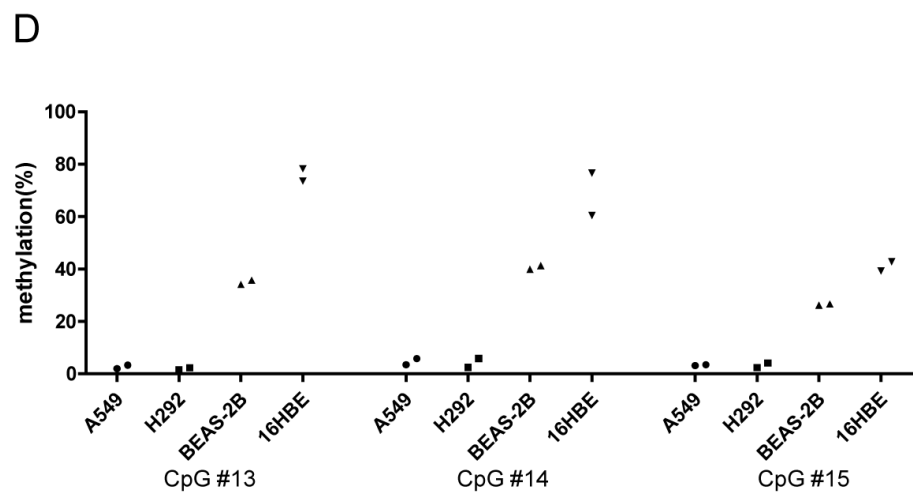
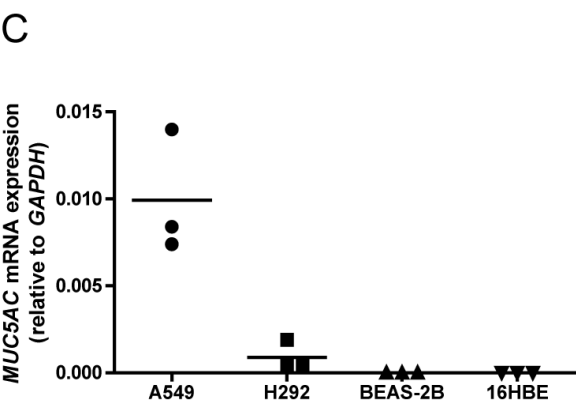
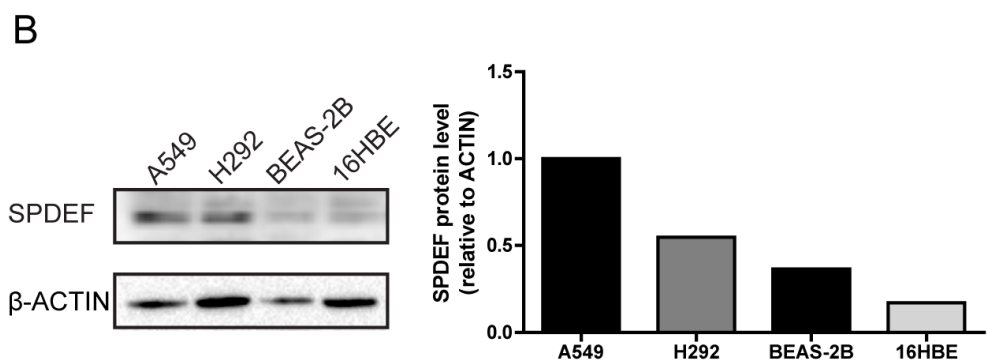
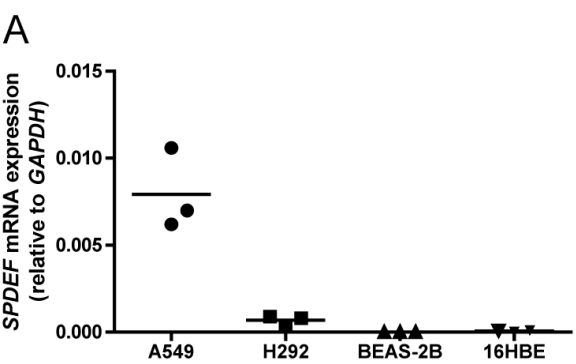
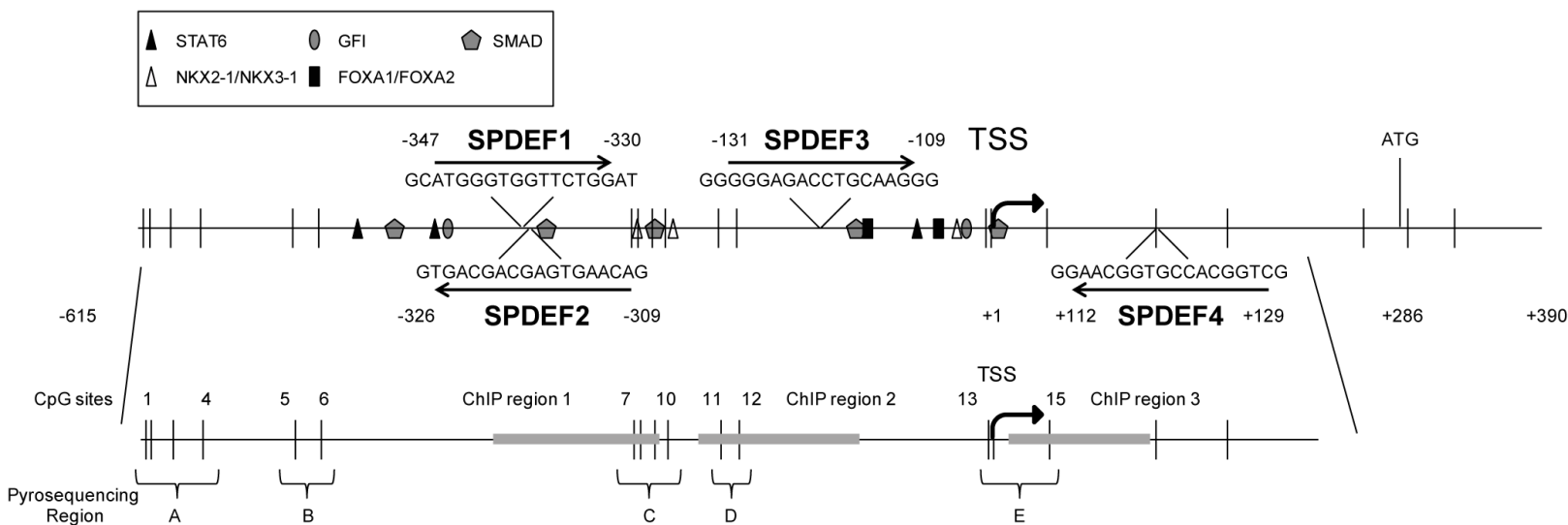
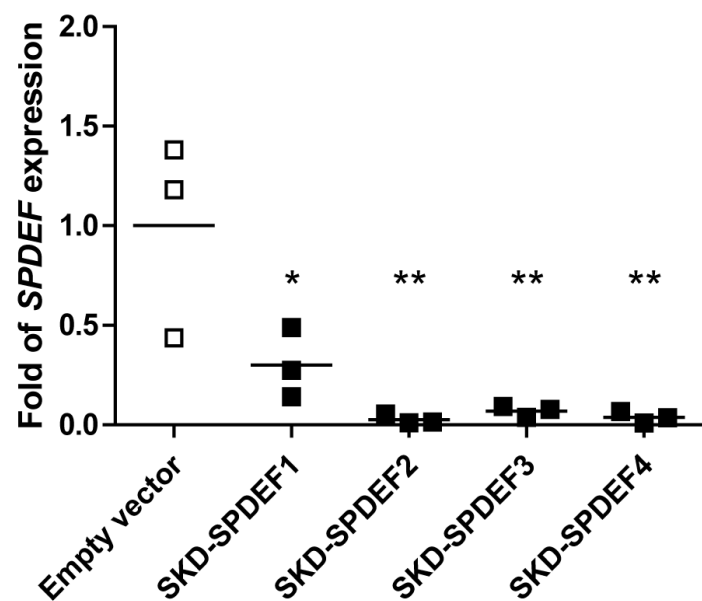


Figure 2

A



B



C

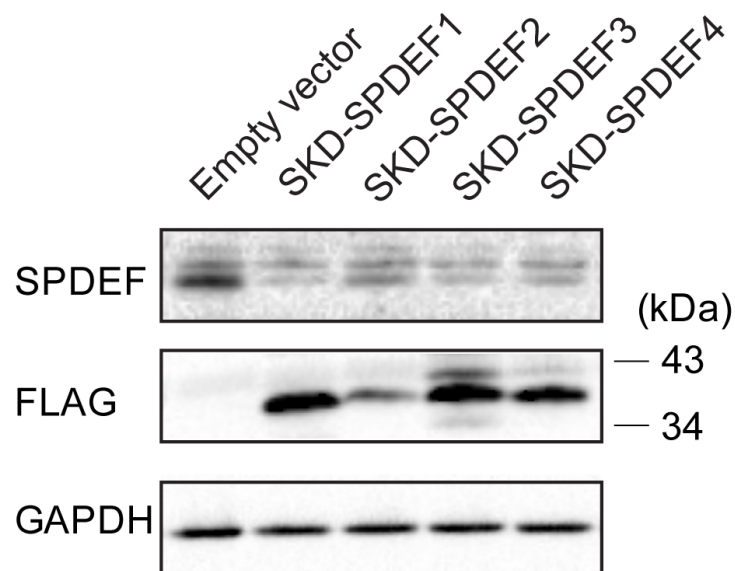


Figure 3

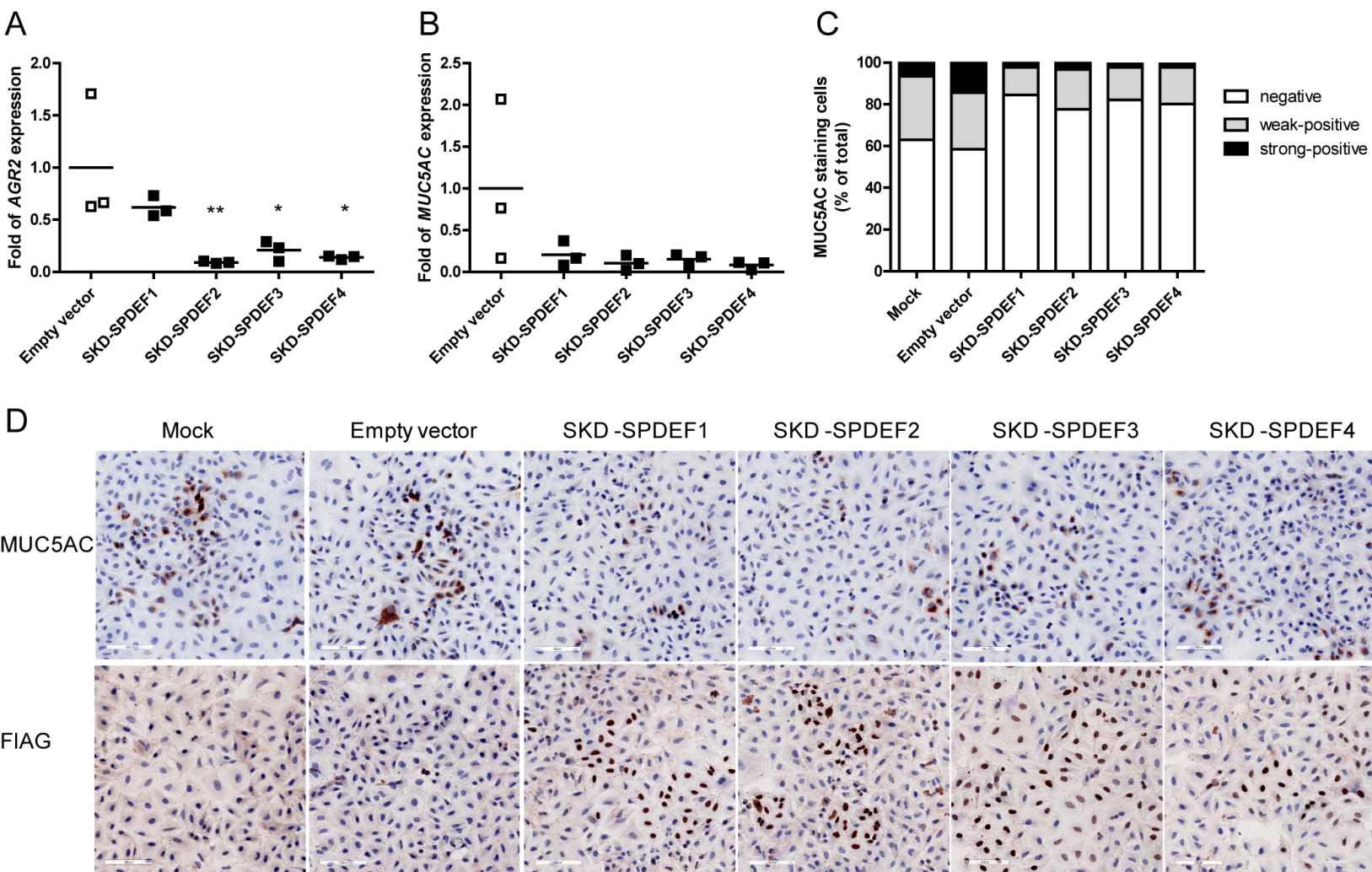


Figure 4

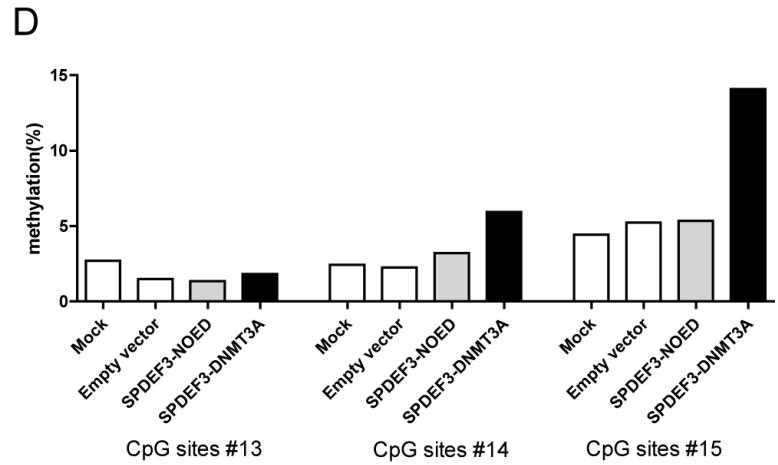
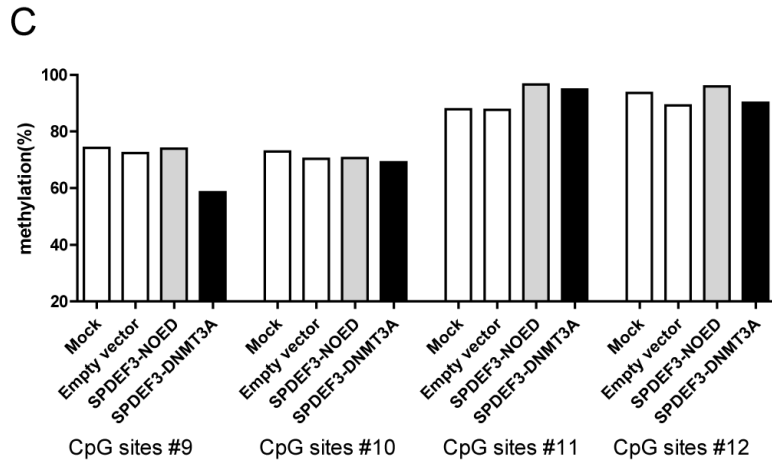
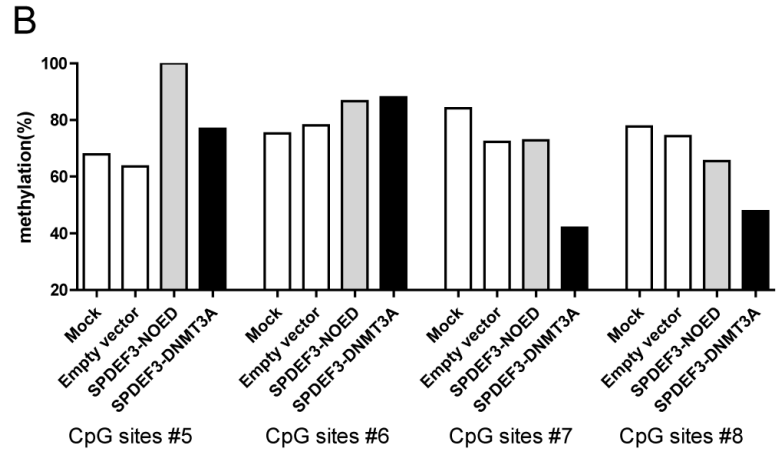
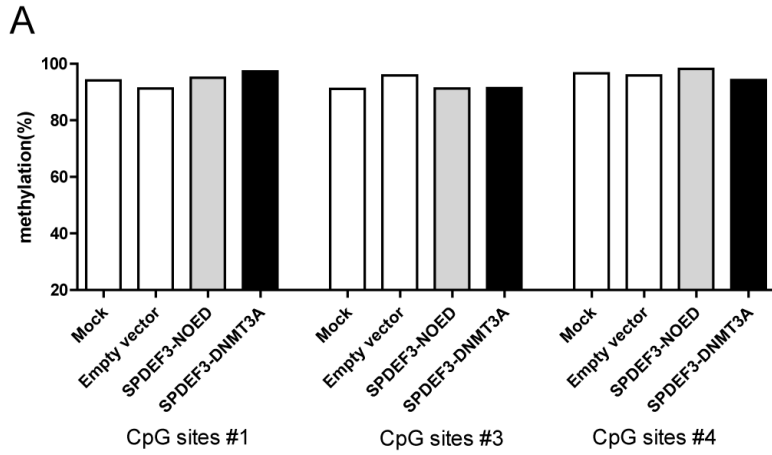
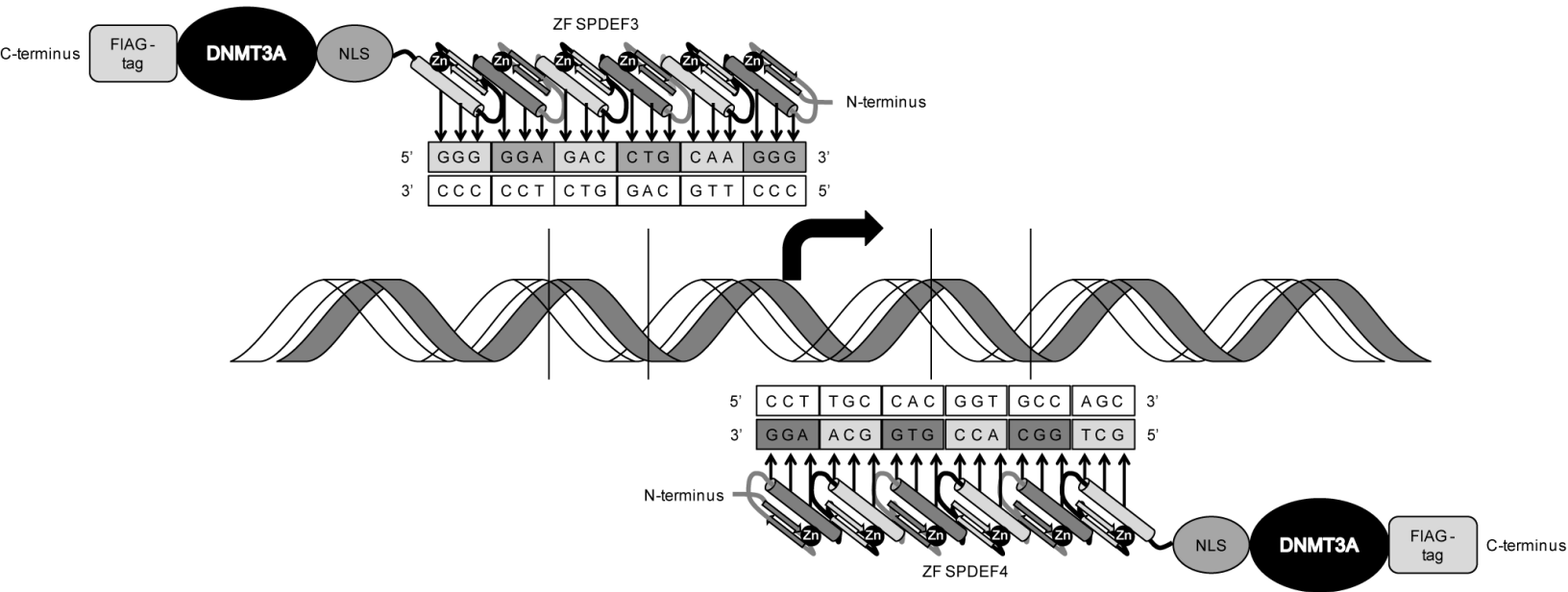
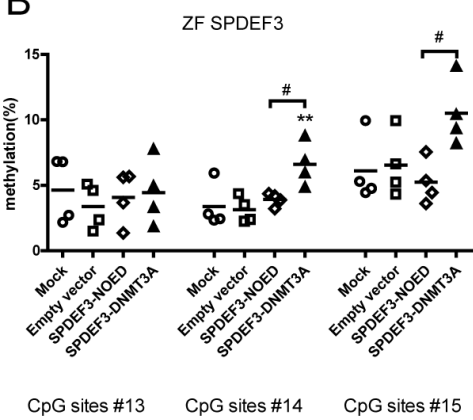


Figure 5

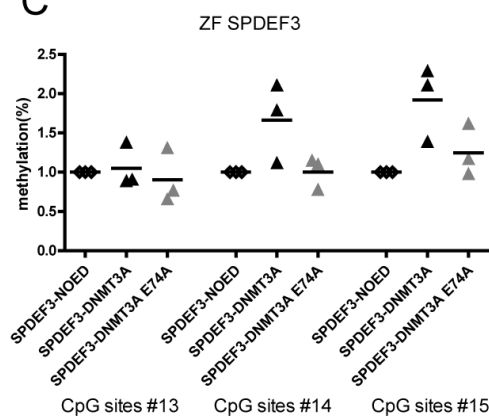
A



B



C



D

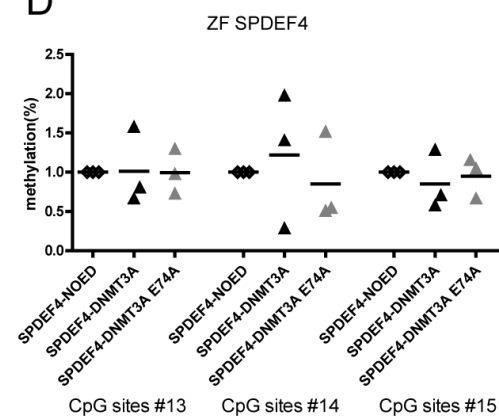
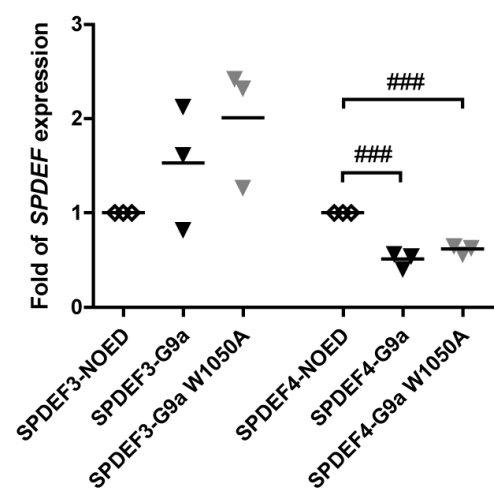
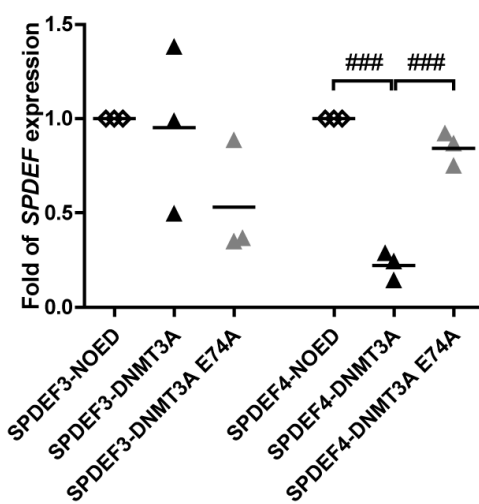
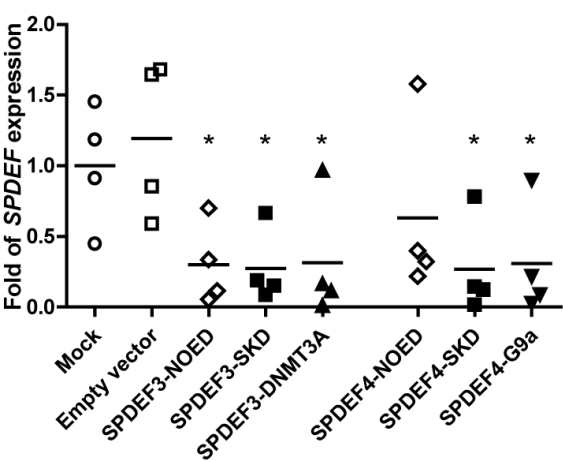
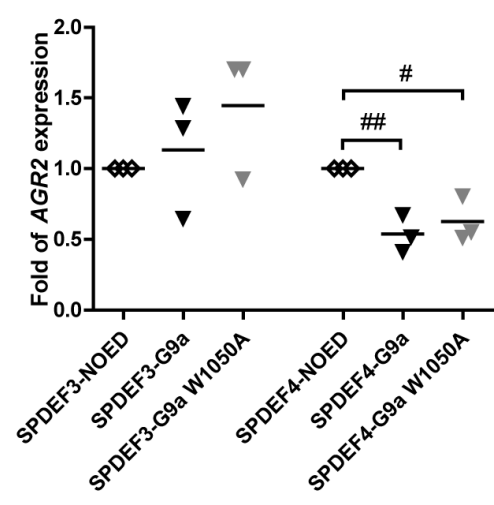
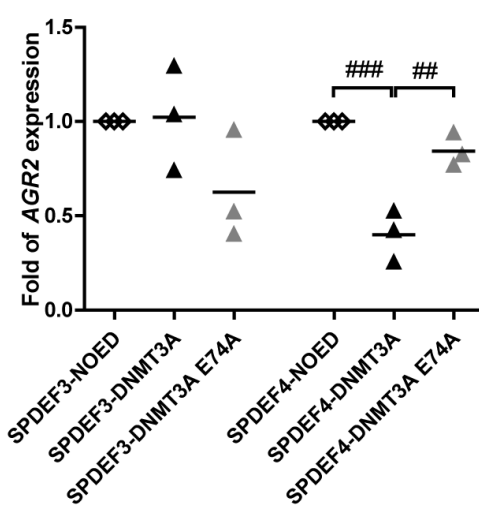
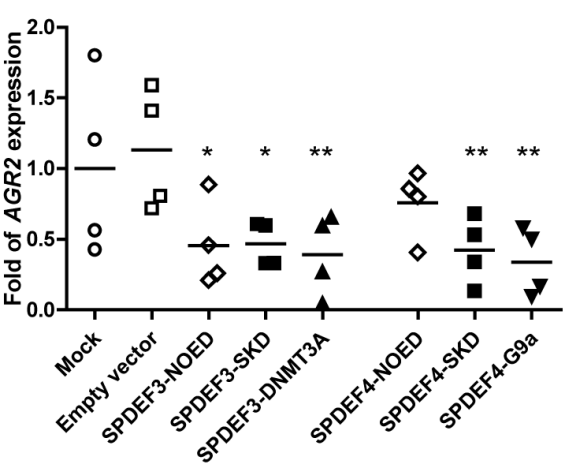


Figure 6

A



B



C

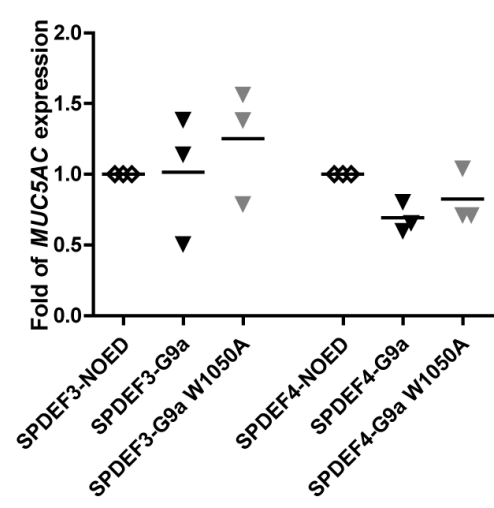
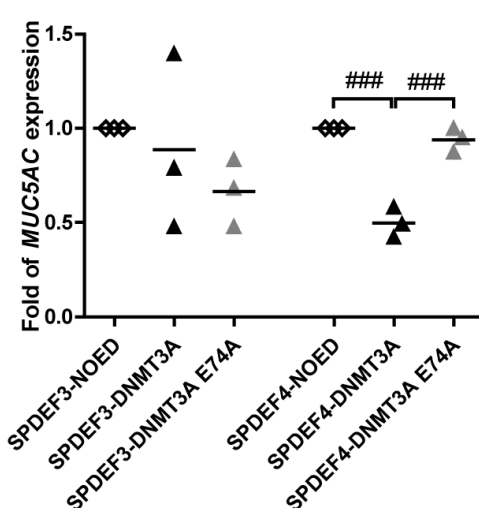
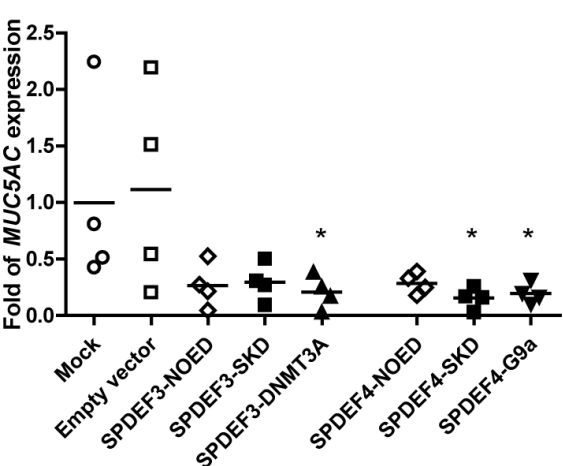
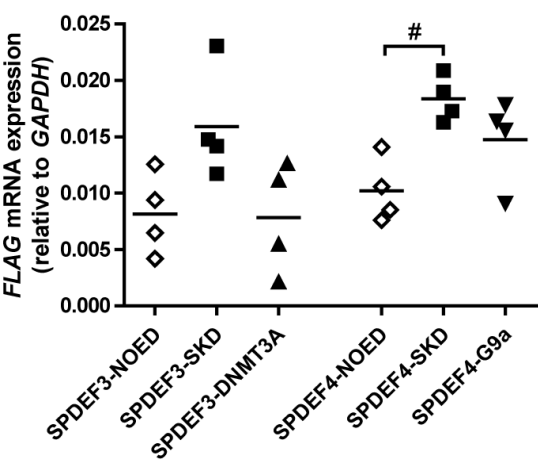
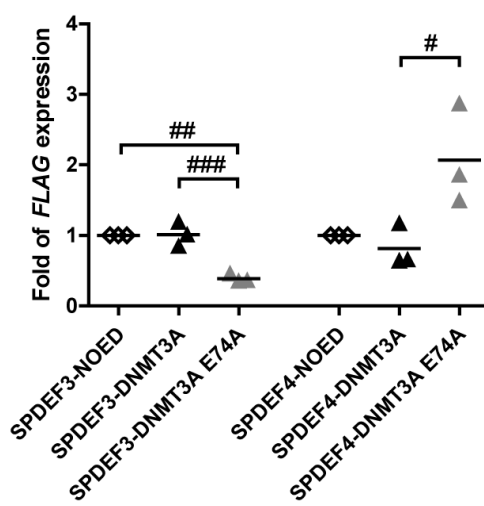


Figure 7

A



B



C

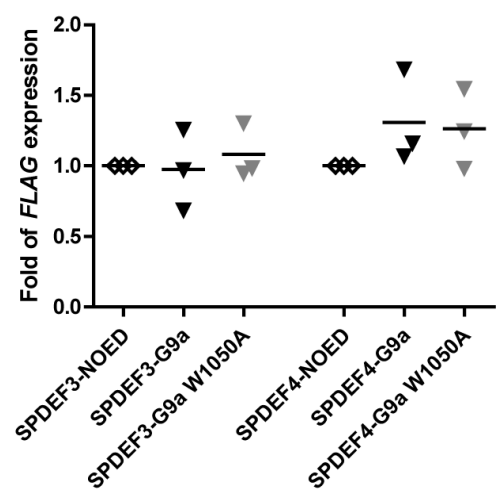
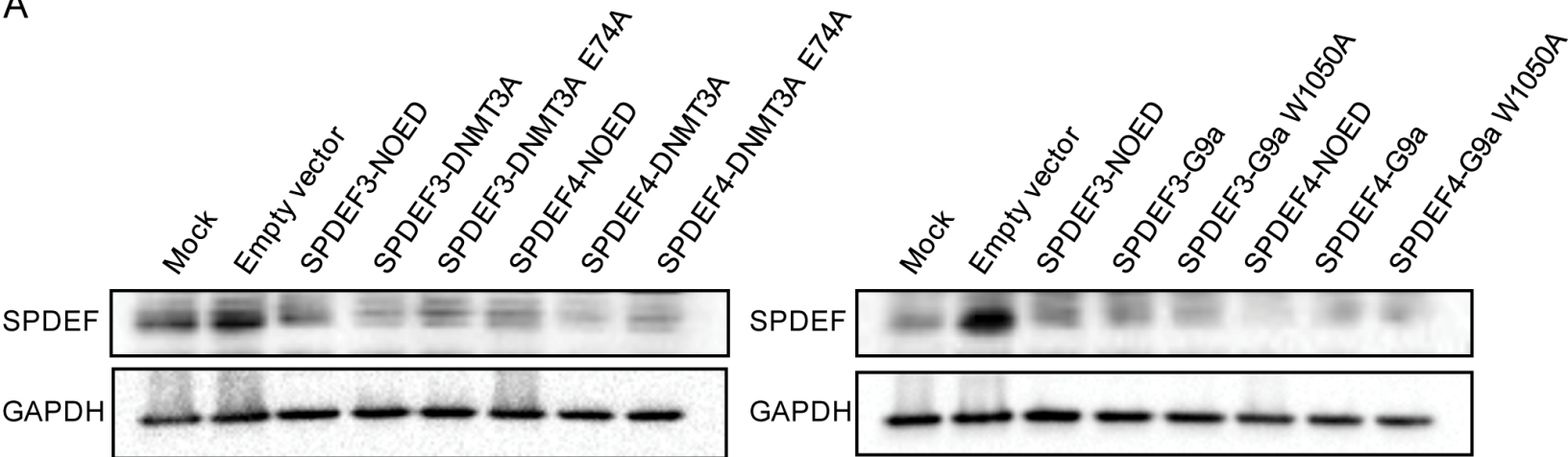


Figure 8

A



B

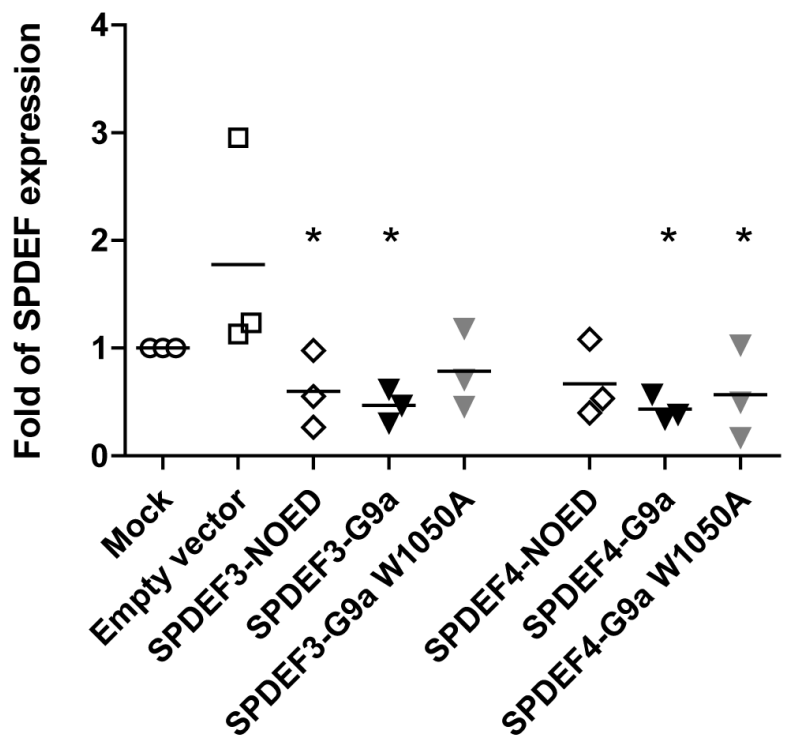
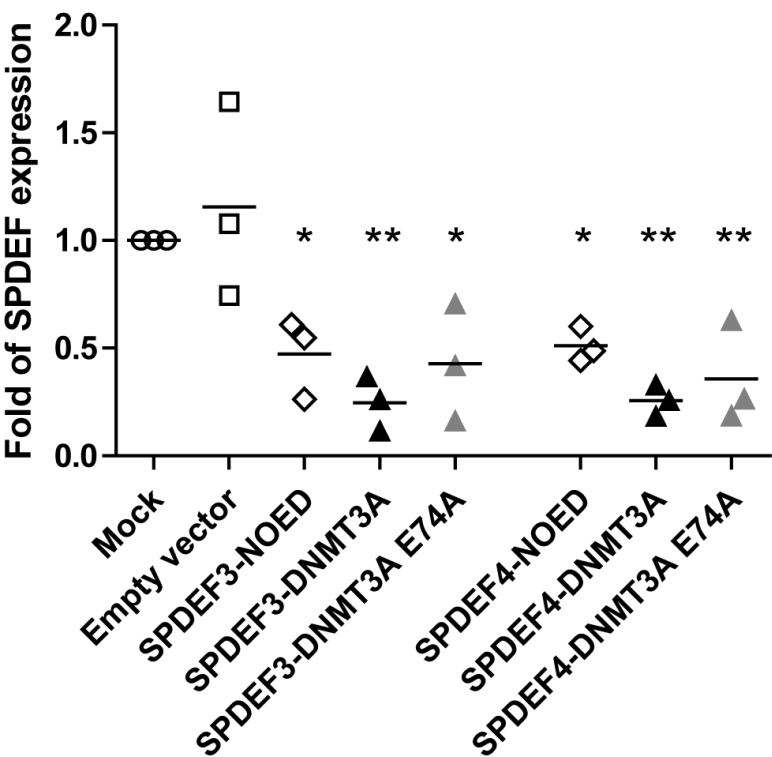
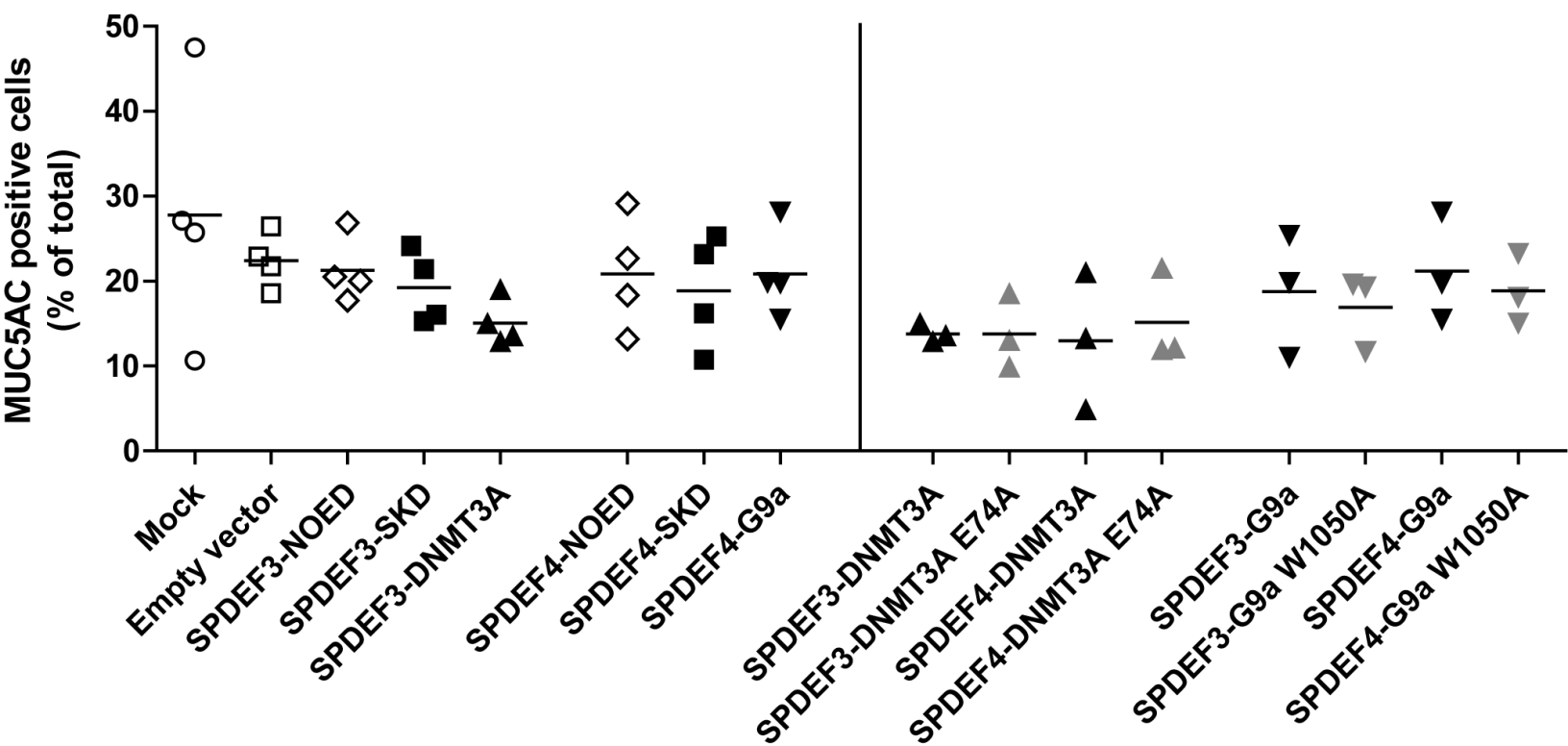


Figure 9

A



B

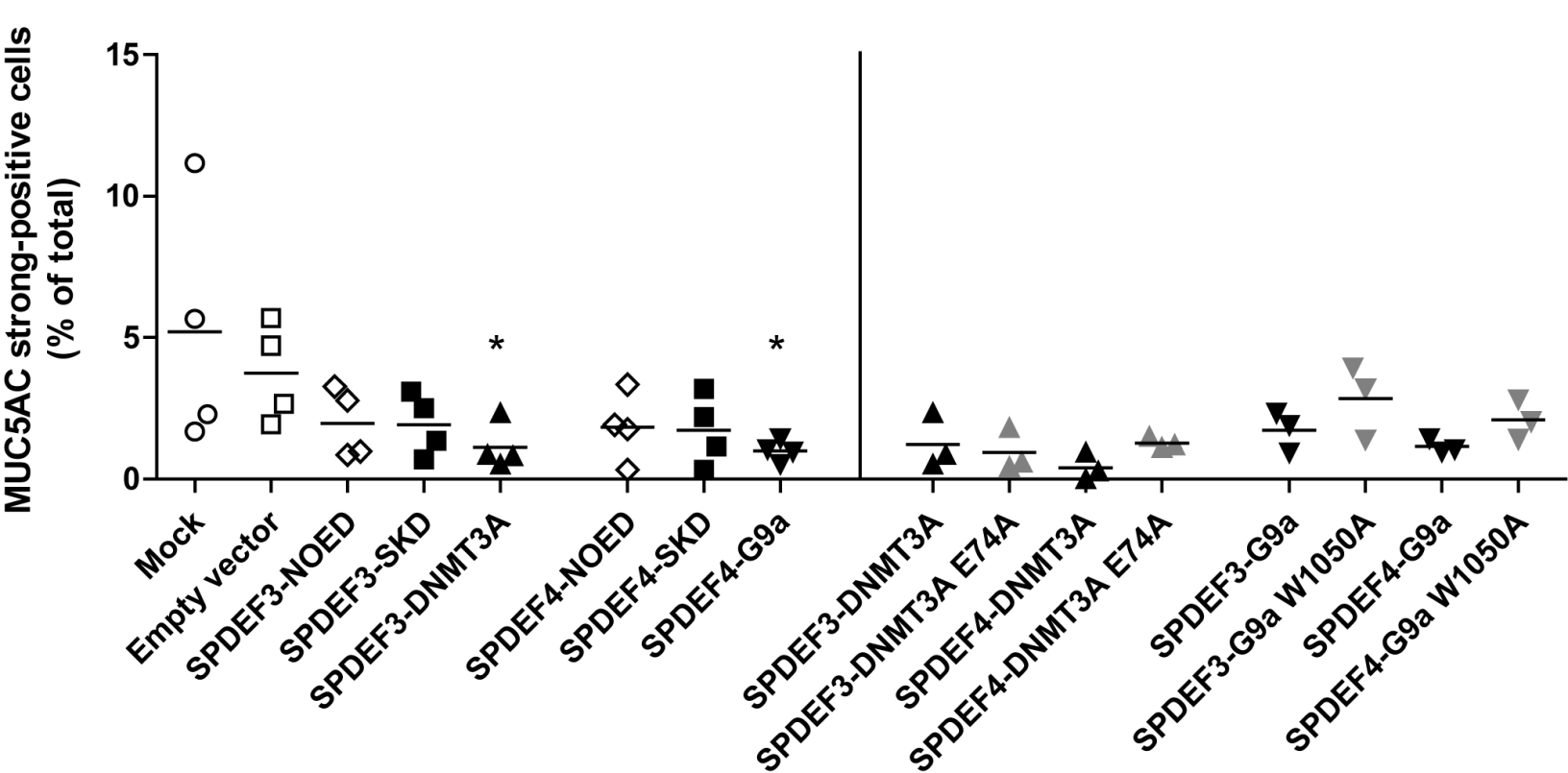
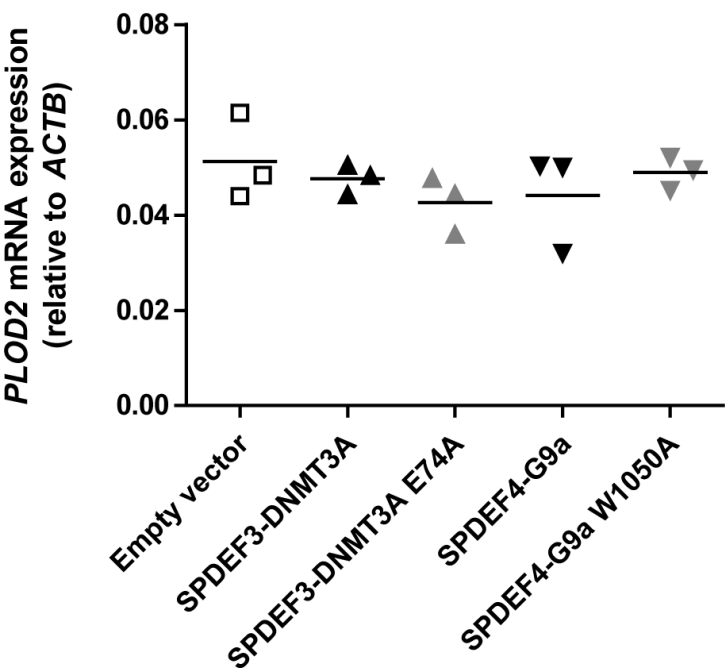
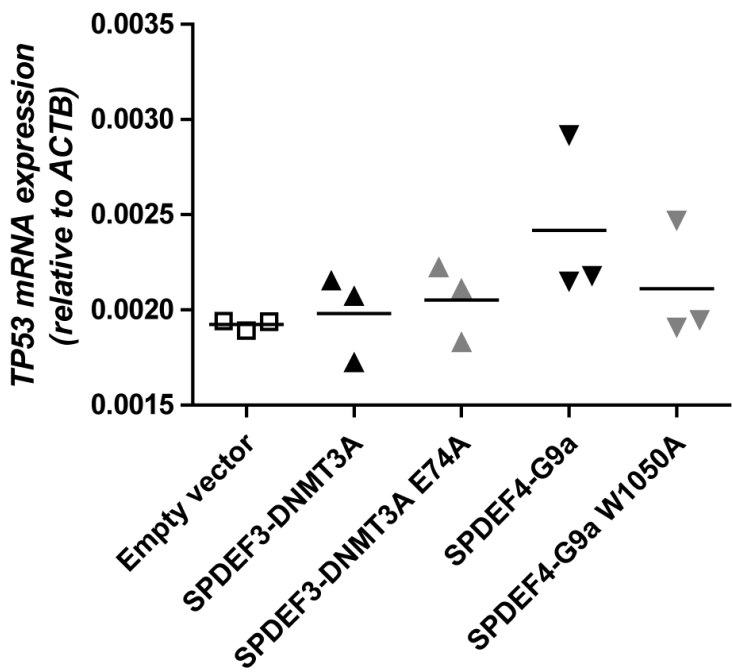


Figure 10

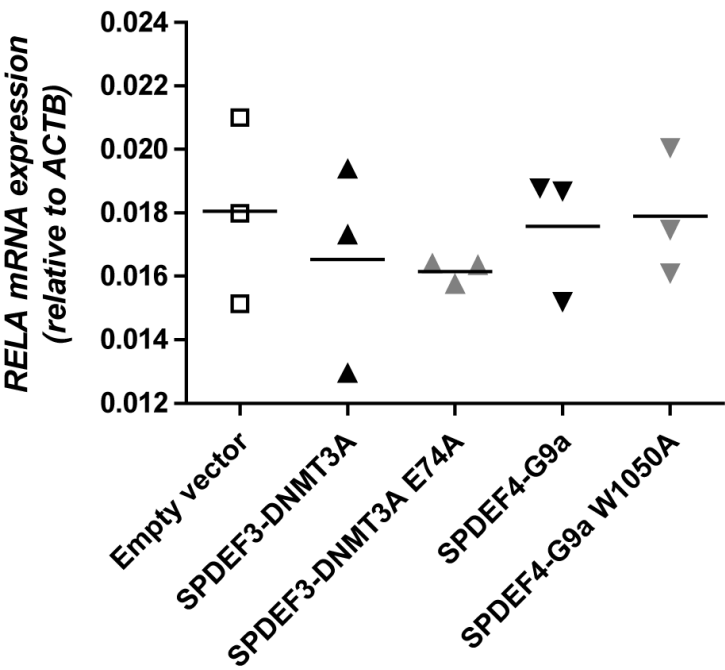
A



B



C



D

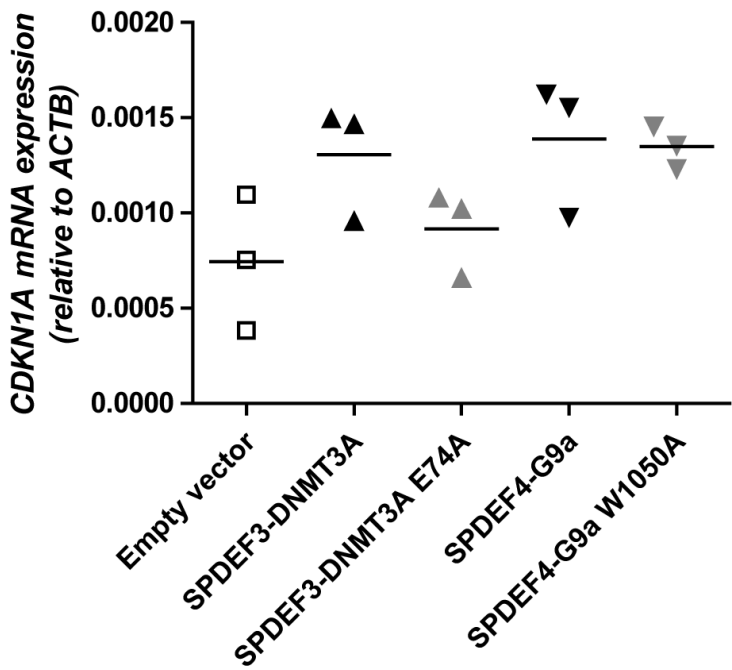
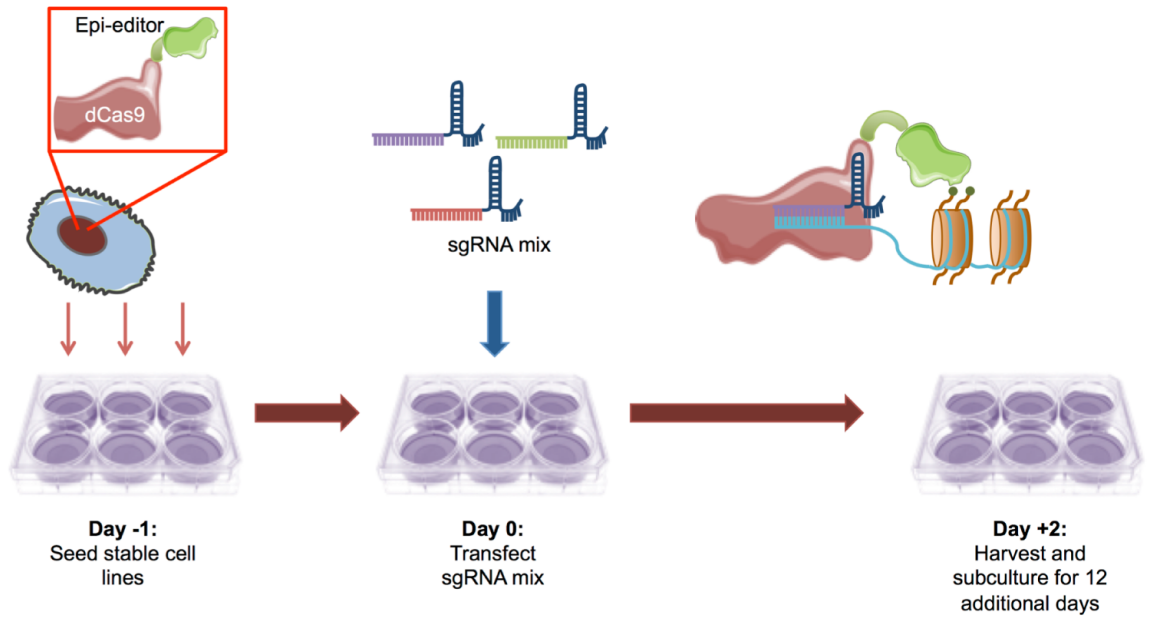
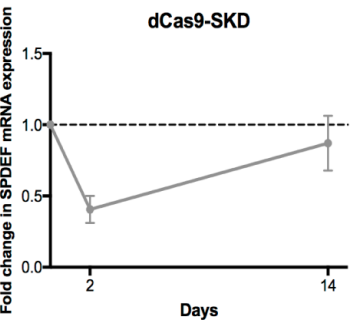


Figure 11

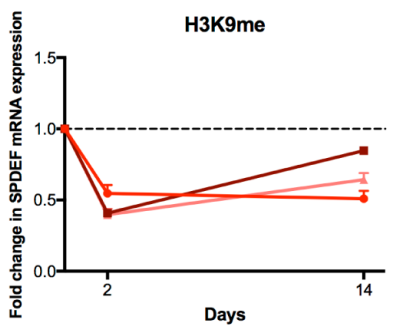
A



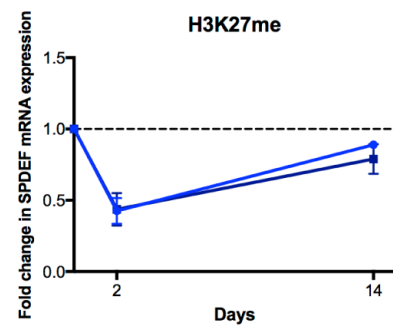
B



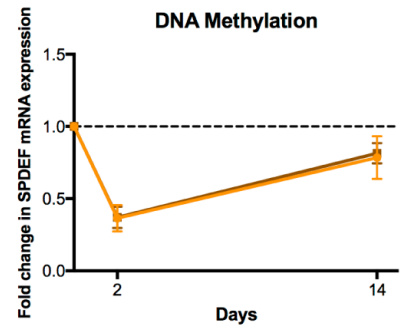
C



D



E



● dCas9-G9a
● dCas9-Mut-G9a
● dCas9-Suv39h1

● dCas9-SET
● dCas9-Mut-SET

● dCas9-3a3L
● dCas9-Mut-3a3L